

ELECTRON-ELECTRON SCATTERING PROCESSES IN QUANTUM WELLS IN A QUANTIZING MAGNETIC FIELD

M.P. Telenkov^{*}, Yu.A. Mityagin^{**}

P.N. Lebedev Physical Institute of the Russian Academy of Sciences, 119991,
Moscow, Russia.

The processes of electron-electron scattering in a quantum well in a quantizing magnetic field are considered. The matrix of electron-electron scattering rates containing all types of transitions is calculated. This matrix is analysed, and the relative magnitude of the rates of transitions of different types is established. The behaviour of electron-electron scattering processes at changing the orientation of the quantising magnetic field is established.

* telenkovmp@lebedev.ru

** mityaginya@lebedev.ru

1. Introduction

A quantizing magnetic field alters the nature of an electron's energy spectrum in a quantum well. Continuous two-dimensional subbands become discrete sets of Landau levels, each exhibiting a high degree of degeneracy with macroscopic multiplicity [1]. This significant transformation in the energy spectrum leads to notable changes in the scattering and relaxation processes [2-15].

In a quantizing magnetic field, the Landau energy exceeds the level broadening, which significantly suppresses one-electron processes of interlevel elastic and quasi-elastic scattering (on impurities, roughness of heterointerfaces, acoustic phonons, etc.). At the same time, the intensity of electron-electron scattering increases due to the high density of states at the Landau levels. As a result, electron-electron scattering becomes the dominant mechanism of redistribution of electrons across Landau levels, which determines the physical picture of relaxation processes [12,15].

Despite the principal role of electron-electron scattering, the electron-electron scattering rate matrix is not well-explored. There are only a few studies [4,12,15] in which several types of transitions due to electron-electron scattering are considered.

There are, however, many more possible kinds of transitions. One of the distinctive features of Landau levels in quantum wells is their equidistant spacing. This equidistance allows for various intrasubband transitions, where the energy conservation law is satisfied regardless of the magnetic field strength. Transitions can occur when electrons are at the same Landau level (Fig. 1a) or different levels. For instance, one type of transition involves an electron from a lower level moving down while another electron from a higher level moves up the Landau level ladder (Fig. 1b). Conversely, another transition occurs when an electron with lower energy ascends while an electron with higher energy descends (Fig. 1c). Additionally, electrons may scatter to neighboring Landau levels or "jump" across multiple levels (Fig. 1d). Among these latter transitions are "crossing transitions," where the electron with lower energy in an interacting pair ends up at a higher position on the Landau level ladder after scattering than the other electron (Fig. 1e).

When Landau levels of different subbands are involved in the electron-electron scattering process, the variety of transitions increases significantly. Transitions are possible when, in the initial state, the electrons of the interacting pair are at one or

different Landau levels of the same subband, and each goes to another subband (Figs. 2a and 2b). Additionally, electron-electron scattering can take place when only one electron moves to a different subband while the other electron traverses the ladder of Landau levels within its initial subband (shown in Fig. 2c). Transitions due to interactions between electrons in different subbands are also possible. In this scenario, the electrons can either pass to different subbands (Fig. 2d) or remain within their original subbands (Fig. 2e).

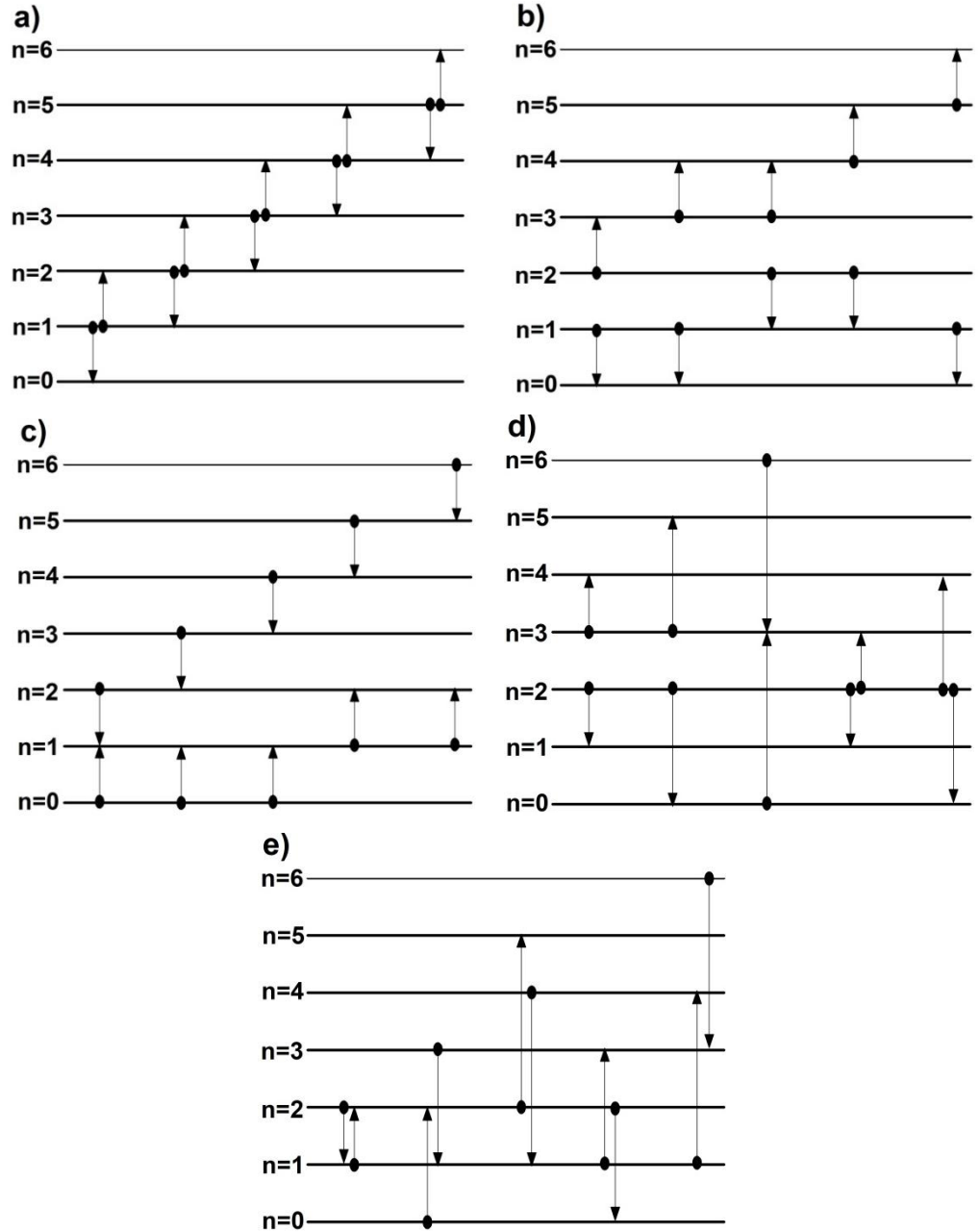


Figure. 1. Different types of interlevel transitions at electron-electron scattering in the Landau level system of one subband.

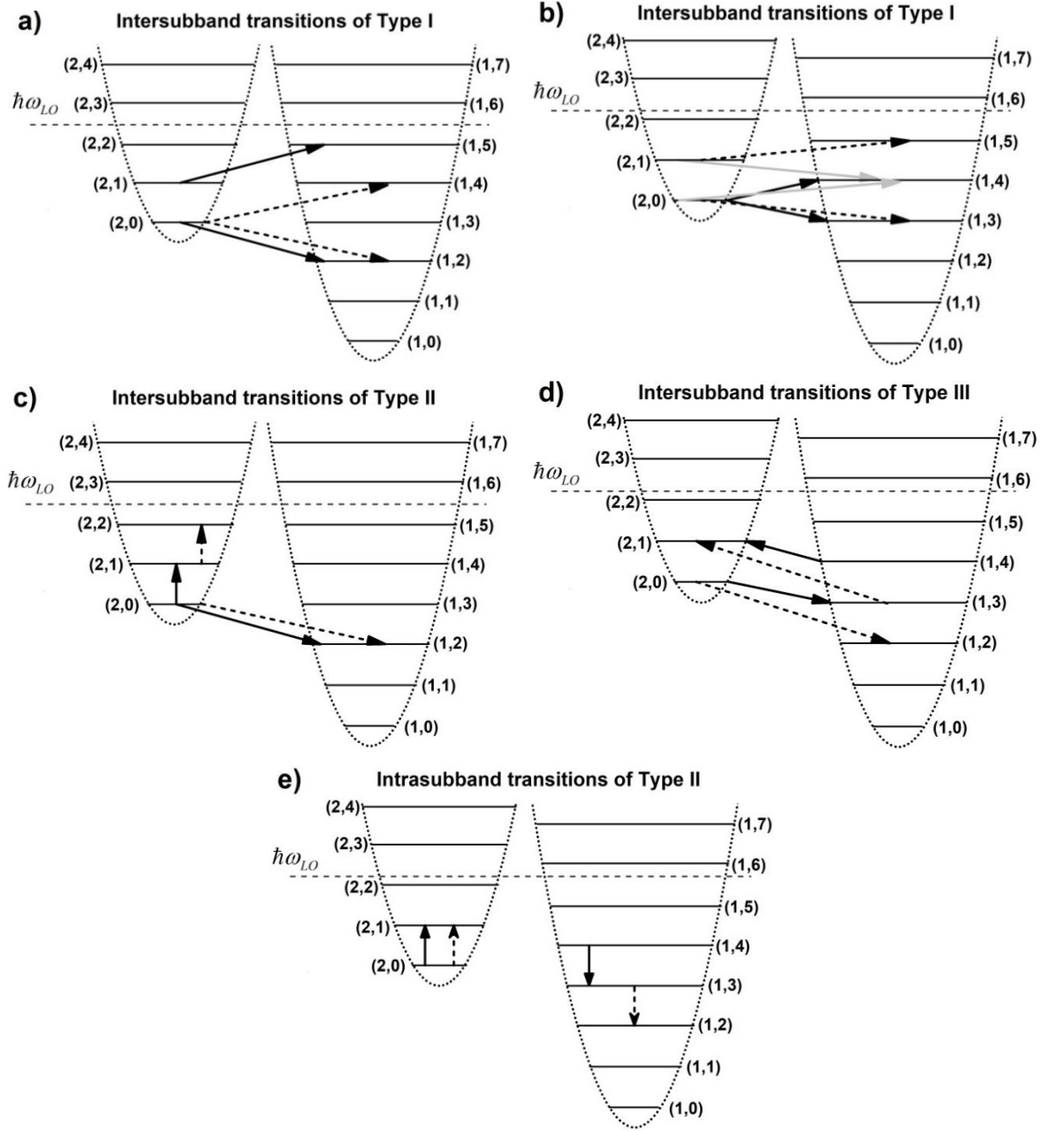


Figure 2: Different types of transitions involving Landau levels of different subbands.

It is important to note that the scattering rate matrix is four-dimensional. Additionally, due to the macroscopically large degeneracy of Landau level in a quantizing magnetic field, each element of this matrix represents a 16-fold integral. Our experience [11-15] in modeling relaxation processes in quantum well structures has demonstrated that hundreds of transitions of various types are necessary to accurately describe electron kinetics. As a result, calculating this matrix is a complex and time-consuming task.

This work aims to analyze the four-dimensional matrix of electron-electron scattering rates and to determine the relative magnitudes of the scattering rates for different types of transitions.

2. Electron spectrum in a quantum well in a quantizing magnetic field

The nature of the magnetic field effect on the electron spectrum depends essentially on its orientation relative to the axis of quantum well growth (the plane of the layers) [16].

When the magnetic field is directed parallel to the layers of the quantum well (perpendicular to the axis of its growth), it does not change the structure of the energy spectrum. The energy spectrum remains a set of continuous two-dimensional subbands. In this case, the magnetic field's influence is reduced to the change of the subband dispersion law [17]. With increasing magnetic field strength, the subband's dispersion law becomes flatter. Only at very high magnetic field values (the magnetic length is much smaller than the width of the quantum well) does the subband transform into a discrete set of Landau levels corresponding to the bulk material. The situation changes substantially when the magnetic field is applied perpendicularly to the layers of the quantum well (along the axis of its growth). In this case, the magnetic field changes the character of the energy spectrum - it transforms each subband into a discrete set of Landau levels [18]:

$$E_{(v,n)} = \varepsilon_v + \hbar \omega_c \left(n + \frac{1}{2} \right), \quad (1)$$

where ε_v - subband energy, $\omega_c = \frac{eB}{mc}$ - cyclotron frequency, $n=0,1,2,3,\dots$ - Landau level number.

Thus, quantization arises precisely when the magnetic field is applied along the growth axis of the structure (perpendicular to its layers). The system of Landau levels in the subband is equidistant. The distance between neighbouring Landau levels in the subband (Landau energy) increases proportionally to the strength of the magnetic field B and, in quantizing magnetic fields, reaches values exceeding the broadening of Landau

levels (for example, in GaAs/Al_{0.3}Ga_{0.7}As quantum wells, the Landau energy is $\hbar\omega_c = 1.72 \cdot B \frac{\text{meV}}{T}$, while the characteristic width of the Landau level is ~ 1 meV).

Landau level degeneracy

$$\alpha = \frac{1}{\pi\ell^2} = \frac{e}{\pi\hbar c} \cdot B = 4.9 \cdot 10^{10} \cdot B \frac{\text{cm}^{-2}}{T} \quad (2)$$

grows linearly with the magnetic field strength and reaches macroscopic values in quantising magnetic fields.

In the case when, in addition to the quantising magnetic field $\mathbf{B}_\perp = B_\perp \mathbf{e}_z$ (z is the axis of the structure growth), a magnetic field $\mathbf{B}_\parallel = B_\parallel \mathbf{e}_y$ parallel to the layers of the quantum well is applied (i.e., the total magnetic field $\mathbf{B} = B_\perp \mathbf{e}_z + B_\parallel \mathbf{e}_y$ is tilted to the plane of the quantum well layers), the Hamiltonian [19] for electron envelope wave-function

$$\hat{H} = \left(\hat{\mathbf{p}} + \frac{e}{c} \mathbf{A} \right) \frac{1}{2m(z)} \left(\hat{\mathbf{p}} + \frac{e}{c} \mathbf{A} \right) + U(z) \quad (3)$$

takes in the Landau gauge $\mathbf{A} = (B_\parallel z - B_\perp y) \mathbf{e}_x$, the form

$$\hat{H} = \hat{\mathbf{p}} \frac{1}{2m(z)} \hat{\mathbf{p}} + U(z) + \frac{m_w}{m(z)} \left[(\omega_\parallel z - \omega_\perp y) \hat{p}_x + \frac{m_w}{2} (\omega_\parallel z - \omega_\perp y)^2 \right]. \quad (4)$$

Here $U(z)$ is the potential profile of the quantum well, $m(z)$ is the effective electron mass (m_w in the well and m_b in the barrier), $\omega_\perp = \frac{eB_\perp}{m_w c}$ and $\omega_\parallel = \frac{eB_\parallel}{m_w c}$ - the cyclotron frequencies for the magnetic field components along the growth axis of the structure (B_\perp) and in the plane of its layers (B_\parallel). respectively.

Since $\hat{H}\hat{p}_x - \hat{p}_x\hat{H} = 0$ then, we can construct a basis of stationary states with a certain momentum projection value on the x-axis. The wave functions of such a basis have the form

$$\Psi(x, y, z) = \frac{\exp(ik_x x)}{\sqrt{L}} \psi(y - k_x \ell_\perp^2, z), \quad (5)$$

where $\ell_\perp = \sqrt{\frac{\hbar}{m\omega_\perp}} = \sqrt{\frac{\hbar c}{eB_\perp}}$ is the magnetic length for the transverse component of the magnetic field. The electron energy levels and wave functions of stationary states are defined by the two-dimensional Hamiltonian [20]

$$\hat{H}_{2D} = \hat{H}_{\perp} + \hat{H}_{\parallel} \quad (6)$$

where

$$\hat{H}_{\perp} = -\frac{\partial}{\partial z} \frac{\hbar^2}{2m(z)} \frac{\partial}{\partial z} + U(z) + \frac{m_w}{m(z)} \left[\frac{\hat{p}_y^2}{2m_w} + \frac{m_w \omega_{\perp}^2}{2} y^2 \right] \quad (7)$$

is the electron Hamiltonian when the magnetic field is directed along the growth axis of the structure. The term

$$\hat{H}_{\parallel} = \frac{m_w}{m(z)} \frac{m_w \omega_{\parallel}^2 z^2}{2} - \frac{m_w}{m(z)} m_w \omega_{\parallel} \omega_{\perp} z y \quad (8)$$

is due to the magnetic field component being parallel to the layers of the quantum well.

The variables in the Schrödinger equation with the Hamiltonian \hat{H}_{\perp} are separable. The energy levels have the form (1), and the wave functions are given by the expression [20]

$$\Psi(x, y, z) = \frac{\exp(ik_x x)}{\sqrt{L}} \varphi_{\nu}(z) \Phi_n(y), \quad (9)$$

where $\varphi_{\nu}(z)$ is the wave-function of the subband energy level ε_{ν} (eigen wave-function of the Hamiltonian $\hat{H}_z = -\frac{\partial}{\partial z} \frac{\hbar^2}{2m(z)} \frac{\partial}{\partial z} + U(z)$), $\Phi_n(y)$ is the wave function of the n-th (n=0,1,2,...) energy level of a linear harmonic oscillator with cyclotron frequency ω_{\perp} .

Note that the relation $m_w / m(z)$ in the third term of the Hamiltonian (7) effectively lowers the barrier height with increasing the Landau level number n by adding to \hat{H}_z the term $-\left(1 - \frac{m_w}{m(z)}\right) \hbar \omega_{\perp} \left(n + \frac{1}{2}\right)$. This leads to a dependence on n of the subband energy levels ε and their wave-functions $\varphi(z)$ [20]. This effect is similar in nature to dimensionality transformation at large wave vector values in quantum wells [21]. However, as it is known, the dependence of the stationary states in a quantum well on the barrier height is significant only for levels close to the continuous spectrum. Therefore, we will further neglect this effect due to its smallness for the lower subbands in the considered sufficiently deep (several hundreds of meV) and wide (more than 5 nm) quantum wells at reasonable values of Landau level numbers.

The matrix of the Hamiltonian (4) in the basis of wave functions (5) is diagonal over k_x , and the matrix element at $k_{x1} = k_{x2}$

$$\begin{aligned} & \left\langle \frac{\exp(ik_x x)}{\sqrt{L}} \psi_1(y - k_x \ell_\perp^2, z) \left| \hat{H} \right| \frac{\exp(ik_x x)}{\sqrt{L}} \psi_2(y - k_x \ell_\perp^2, z) \right\rangle = \\ & = \langle \psi_1(y, z) | \hat{H}_{2D} | \psi_2(y, z) \rangle \end{aligned} \quad (10)$$

does not depend on k_x . Therefore, in the tilted quantising magnetic field, the Landau level degeneracy is determined only by the quantising component B_\perp of the magnetic field and is given by the expression

$$\alpha = \frac{e}{\pi \hbar c} \cdot B_\perp. \quad (11)$$

The matrix element between the Landau level (ν_1, n_1) and (ν_2, n_2) is given by the expression [22]

$$\begin{aligned} & \langle \nu_1, n_1 | \hat{H}_{2D} | \nu_2, n_2 \rangle = \left[\varepsilon_{\nu_1} + \hbar \omega_\perp (n + 1/2) \right] \delta_{\nu_1, \nu_2} \delta_{n_1, n_2} + \\ & + \frac{m_w \omega_\parallel^2}{2} \langle z^2 \rangle_{\nu_1, \nu_2} \delta_{n_1, n_2} - m_w \hbar \omega_\parallel \sqrt{\hbar \omega_\perp} \sqrt{\frac{m_w}{2 \hbar^2}} \langle z \rangle_{\nu_1, \nu_2} \times \\ & \times \left[\sqrt{n_2 + 1} \cdot \delta_{n_1, n_2 + 1} + \sqrt{n_2} \cdot \delta_{n_1, n_2 - 1} \right] \end{aligned} \quad (12)$$

In a quantum well in a tilted magnetic field, there are two scales of energies - cyclotron energy and intersubband spacing. We will be interested in the case when the cyclotron energy is several times smaller than the intersubband spacing. In this case, in matrix (12), we can neglect the coupling between subbands (elements with $\nu_1 \neq \nu_2$) and diagonalize it analytically [23-26]. As a result, the following expressions for the Landau levels and wave functions of stationary states are obtained

$$E_{(\nu, n)} = \varepsilon_\nu + \delta \varepsilon_\nu(B_\parallel) + \hbar \omega_\perp \left(n + \frac{1}{2} \right) \quad (13)$$

and

$$\Psi(x, y, z) = \frac{\exp(ik_x x)}{\sqrt{L}} \varphi_\nu(z) \Phi_n(y - k_x \ell_\perp^2 - \langle z \rangle_\nu \tan \theta). \quad (14)$$

Here

$$\delta \varepsilon_\nu(B_\parallel) = \frac{m_w \omega_\parallel^2}{2} (\delta z)_\nu^2 = \frac{e^2}{2 m_w c^2} (\delta z)_\nu^2 \cdot B_\parallel^2. \quad (15)$$

$$\langle z \rangle_v = \int dz \varphi^*(z) z \varphi(z) \quad (16)$$

is the mean value of the electron z-coordinate, $(\delta z)_v$ - its standard deviation, θ - tilted magnetic field angle to the quantum well's growth axis ($\tan \theta = \frac{B_{\parallel}}{B_{\perp}}$).

As can be seen, the Landau quantization is caused only by the magnetic field component B_{\perp} perpendicular to the layers of the heterostructure.

The component B_{\parallel} does not lead to the quantization of the electron energy. Its main effect on the energy spectrum is to shift each subband by an amount proportional to B_{\parallel}^2 and $(\delta z)_v^2$ in the states of the given subband. The B_{\parallel} also leads to the fact that the magnetic component of the wave-function becomes dependent on the subband wave-function – there is a shift of the centre of the linear harmonic oscillator by the value of $\langle z \rangle_v \tan \theta$, proportional to B_{\parallel} .

3. Electron-electron scattering rate matrix

It is necessary to calculate the electron fluxes between levels to describe the kinetics of electrons in the Landau level system. In particular, these fluxes define a system of rate equations [7-15]

$$\frac{dN_i}{dt} = \sum_{j,f,g} J_{e-e} \begin{pmatrix} f & g \\ i & j \end{pmatrix} - \sum_{j,f,g} J_{e-e} \begin{pmatrix} i & j \\ f & g \end{pmatrix} + \text{single particle processes}. \quad (17)$$

Here N_i is the number of electrons at the Landau level $i = (\nu_i, n_i)$, related to the unit area L^2 of the quantum well cross-section (the population of the Landau level).

In the Fermi rule approximation, the intensity (the number of scattering acts per unit time per unit area of the cross-section) of the transition when one electron transitions from the Landau level i to the Landau level f , and the other from the Landau level j to the Landau level g (transition $\{(\nu_i, n_i) \rightarrow (\nu_f, n_f); (\nu_j, n_j) \rightarrow (\nu_g, n_g)\}$) is given by the expression [4,9]

$$J \begin{pmatrix} i & j \\ f & g \end{pmatrix} = W_{e-e} \begin{pmatrix} i & j \\ f & g \end{pmatrix} \cdot N_i N_j \left[1 - \frac{N_g}{\alpha} \right] \left[1 - \frac{N_f}{\alpha} \right], \quad (18)$$

where

$$W_{e-e} \begin{pmatrix} i & j \\ f & g \end{pmatrix} = A_{e-e} \begin{pmatrix} i & j \\ f & g \end{pmatrix} \times F_{e-e} (E_i + E_j - E_f - E_g) \quad (19)$$

is the element of the electron-electron scattering rate matrix corresponding to this transition,

$$\begin{aligned} A_{e-e} \begin{pmatrix} i & j \\ f & g \end{pmatrix} &= \frac{8\pi}{\hbar} \frac{1}{L^2} \sum_{k_i} \sum_{k_j} \sum_{k_f} \sum_{k_g} \left| V_{(i,f)(g,j)}^{e-e} (k_i, k_f, k_j, k_g) \right|^2 \cdot \frac{1}{\alpha^2} = \\ &= \frac{L^2}{2\pi^3 \hbar \alpha^2} \int dk_i dk_j dk_f dk_g \left| V_{(i,f)(g,j)}^{e-e} (k_i, k_f, k_j, k_g) \right|^2 \end{aligned} \quad (20)$$

is the amplitude of the transition,

$$\begin{aligned} V_{(i,f)(g,j)}^{e-e} (k_i, k_f, k_j, k_g) &= \int d\mathbf{r}_1 d\mathbf{r}_2 \Psi_{(f,k_f)}^* (\mathbf{r}_1) \Psi_{(g,k_g)}^* (\mathbf{r}_2) \times \\ &\times \frac{e^2}{\varepsilon |\mathbf{r}_1 - \mathbf{r}_2|} \Psi_{(i,k_i)} (\mathbf{r}_1) \Psi_{(j,k_j)} (\mathbf{r}_2) \end{aligned} \quad (21)$$

ε_s - static dielectric constant,

$$\begin{aligned} F_{e-e} (E_i + E_j - E_f - E_g) &= \int dE_1 dE_2 dE_3 dE_4 \rho_{i,k_i} (E_1) \rho_{f,k_f} (E_2) \times \\ &\times \rho_{j,k_j} (E_3) \rho_{g,k_g} (E_4) \cdot \delta (E_1 + E_3 - E_2 - E_4) \end{aligned} \quad (22)$$

is the transition form-factor, taking into account the finite broadening of Landau levels. Following [1,27,28], the single-particle density of states is approximated by the Gaussian

$$\rho_{i,k_i} (E) = \frac{1}{\sqrt{2\pi}\Gamma} \exp \left(-\frac{(E - E_i)^2}{2\Gamma^2} \right). \quad (23)$$

with the width $\Gamma = 1$ meV, typical for the considered structures and magnetic fields. In this case, the form factor (20) is also Gaussians

$$\begin{aligned} F_{(i,f)(j,g)}^{e-e} (k_i, k_f, k_j, k_g) &= \frac{1}{\sqrt{2\pi}\Gamma_{\Sigma}^{ee}} \exp \left\{ -\frac{(E_i + E_j - E_f - E_g)^2}{2(\Gamma_{\Sigma}^{ee})^2} \right\} \equiv \\ &\equiv F_{ee} (E_i + E_j - E_f - E_g) \end{aligned} \quad (24)$$

with a maximum corresponding to the energy conservation law in electron-electron scattering $E_i + E_j = E_g + E_f$ and a (transition) width $\Gamma_{ee}^{\Sigma} = \sqrt{4\Gamma^2} = 2\Gamma$ meV.

As can be seen, the scattering rate amplitude is a multiple integral with a Coulomb singularity, which makes its calculation a rather complicated and time-consuming task

and, to all appearances, is the reason for the scanty information on the rate matrix in the literature.

Using the wave-functions (14), we could perform analytically an integration in (20) and thereby substantially lower the multiplicity of the integral. As a result, we obtained the following expression for the electron-electron scattering amplitude

$$A_{e-e} \begin{pmatrix} i & j \\ f & g \end{pmatrix} = \frac{4e^4}{\pi^2 \varepsilon_s^2 \hbar} \frac{\exp \left(\left[-\frac{(\xi_{v_f, v_i} + \xi_{v_g, v_j})^2}{4} \right] \right)}{2^{n_i + n_j + n_g + n_f} n_i! n_j! n_g! n_f!} \times \quad (25)$$

$$\times \iint dk_1 dk_2 \exp \left(- \left[k_2 - \frac{(\xi_{v_i, v_j} + \xi_{v_g, v_f})}{2} \right]^2 \right) |M_{i,j,g,f}(k_1, k_2)|^2$$

where

$$M_{i,j,g,f}(k_1, k_2) = \int dy \exp \left(-\frac{1}{2}(y + k_1 - k_2)^2 \right) \times \quad (26)$$

$$\times G_{v_i, v_j, v_g, v_f} \left(|k_2|; \left| y + \frac{\xi_{v_i, v_j} + \xi_{v_g, v_f}}{2} \right| \right) \Lambda_{n_i, n_j, n_g, n_f}(k_2, y + k_1 - k_2)$$

$$G_{v_i, v_j, v_g, v_f}(\gamma; y) = \int dz_1 K_0 \left(\gamma \sqrt{y^2 + \frac{4z_1^2}{\ell_\perp^2}} \right) \times R_{v_i, v_j, v_g, v_f}(z_1), \quad (27)$$

$$R_{v_i, v_j, v_g, v_f}(z_1) = \int dz_2 \phi_{v_i}(z_2) \phi_{v_j}(z_2 - 2z_1) \phi_{v_g}^*(z_2 - 2z_1) \phi_{v_f}^*(z_2), \quad (28)$$

$$\Lambda_{n_i, n_j, n_g, n_f}(k, y) = 2^{\frac{n_i + n_j + n_g + n_f}{2}} \sqrt{2} \sum_{p_1=0}^{n_i} \frac{1}{2^{p_1/2}} \binom{n_i}{p_1} H_{p_1}(\delta_i) \sum_{p_2=0}^{n_j} \frac{1}{2^{p_2/2}} \binom{n_j}{p_2} H_{p_2}(\delta_j) \times \quad (29)$$

$$\times \sum_{p_3=0}^{n_g} \frac{1}{2^{p_3/2}} \binom{n_g}{p_3} H_{p_3}(\delta_g) \times \sum_{p_4=0}^{n_f} \frac{1}{2^{p_4/2}} \binom{n_f}{p_4} H_{p_4}(\delta_f) \times$$

$$\times \frac{\left[1 + (-1)^{n_i + n_j + n_g + n_f - p_1 - p_2 - p_3 - p_4} \right]}{2} \times$$

$$\times \Gamma \left(\frac{n_i + n_j + n_g + n_f - p_1 - p_2 - p_3 - p_4}{2} + \frac{1}{2} \right),$$

$K_0(x)$ - McDonald function, $\Gamma(x)$ - Euler gamma function, $H_n(x)$ - Hermite polynomial of degree n,

$$\delta_i = \frac{y + k + \xi_{v_f, v_i}}{2}, \quad (30)$$

$$\delta_j = \frac{-y - k + \xi_{\nu_g, \nu_j}}{2}, \quad (31)$$

$$\delta_g = \frac{-y + k - \xi_{\nu_g, \nu_j}}{2}, \quad (32)$$

$$\delta_f = \frac{y - k - \xi_{\nu_f, \nu_i}}{2}. \quad (33)$$

$$\xi_{\nu_1, \nu_2} = \sqrt{\frac{e}{\hbar c B_\perp}} \cdot \left[\langle z \rangle_{\nu_1} - \langle z \rangle_{\nu_2} \right] \cdot B_\parallel \quad (34)$$

Note that, in addition to a significant decrease in the multiplicity of the integral, the obtained expression has many advantages for numerical calculations. First, all information about the heterostructure is contained in only one integral, namely the integral (28), through the subband wave functions $\varphi(z)$. Moreover, this integral is defined only by $\varphi(z)$ and does not include the components of the wave function (14) along other coordinate axes. Therefore, the function $R_{\nu_i, \nu_j, \nu_g, \nu_f}(z_1)$ defined by (28) is the same for all transitions between fixed subbands ν_i, ν_j, ν_g and ν_f in a given heterostructure. Accordingly, it can be calculated only once and used for all transitions with possible combinations of n_i, n_j, n_g and n_f at any magnetic field magnitude. In essence, this decreases by 1 the multiplicity of integration. In addition, for many widely used heterostructures (in particular, for the rectangular quantum well), analytical expressions for the wave functions $\varphi(z)$ of the subbands are known, which makes it possible to calculate the integral (28) analytically.

The function $G_{\nu_i, \nu_j, \nu_g, \nu_f}(\gamma; y)$, defined by the integral (27), is also determined only by the subband wave functions and is the same for all transitions between fixed subbands ν_i, ν_j, ν_g and ν_f of a given heterostructure, which allows it to be calculated only once, using then for all transitions with all possible combinations of n_i, n_j, n_g and n_f . However, unlike the integral (28), the integrand function in (27) depends on the magnetic length of the magnetic field component B_\perp .

4. Intra-subband transitions

This section presents the results of the study of intrasubband electron-electron scattering processes. The obtained regularities are illustrated in the example of the lower ($\nu=1$) subband of the GaAs/Al_{0.3}Ga_{0.7}As quantum well with a width of 25 nm.

As discussed in Section 2, all the main features of the electronic spectrum in the considered system, distinguishing it from other electronic systems, are due to the magnetic field component directed along the growth axis of the heterostructure. Therefore, to emphasize the role of these features as clearly as possible, let us first consider the scattering processes in the magnetic field directed perpendicularly to the layers of the heterostructure.

Electron-electron scattering is an elastic two-particle process. For the transition $\{(\nu_i, n_i) \rightarrow (\nu_f, n_f) \& (\nu_j, n_j) \rightarrow (\nu_g, n_g)\}$, the energy conservation law (the transition resonance condition) has the form

$$E_{(\nu_i, n_i)} + E_{(\nu_j, n_j)} = E_{(\nu_f, n_f)} + E_{(\nu_g, n_g)}. \quad (35)$$

Substitution in (35) of the expression (13) for the single-particle energy gives

$$n_f - n_i + n_g - n_j = \frac{(\varepsilon_{\nu_i} - \varepsilon_{\nu_f} + \varepsilon_{\nu_j} - \varepsilon_{\nu_g})}{\hbar\omega_c}. \quad (36)$$

For intrasubband transitions $\nu_i = \nu_j = \nu_g = \nu_f$ and, respectively, the resonance condition (36) takes the form

$$n_f - n_i + n_g - n_j = 0. \quad (37)$$

Thus, the equidistance of the one-electron spectrum of a subband leads to the fact that the resonance condition (the energy conservation law) for intrasubband processes does not depend on the magnetic field. As a result, the intrasubband electron-electron scattering rates decrease monotonically and slowly with increasing magnetic field.

The above is illustrated by Figure 3, which shows a typical dependence of the intrasubband scattering rate on the magnetic field. The slight decrease of the scattering rate can be explained by the fact that with increasing magnetic field, the magnetic length, which defines the localization region of the wave-function, decreases (the RMS deviation of the coordinate at the n -th level of the linear harmonic oscillator is equal to $\ell\sqrt{n+1/2}$, $\ell = \sqrt{\hbar c / eB}$ is the magnetic length). Consequently, the interacting electron wave-

function overlapping in the plane of layers goes low, and the scattering probability decreases. Since the magnetic length changes relatively slowly with the magnetic field ($\sim 1/\sqrt{B}$), lowering the electron-electron scattering rate with increasing magnetic field is relatively slow.

Thus, at any magnetic field value, the subband has numerous transitions, for each of which the energy conservation law is satisfied. Three numbers can describe this rich set of transitions, and the following general formula for intrasubband transitions can be written as follows:

$$\{n \rightarrow n - \Delta n \ \& \ n + \Delta N \rightarrow n + \Delta N + \Delta n\}, \quad (38)$$

The subband number ν , which is the same for all levels, is omitted. Here, n is the number of the Landau level from which the electron of the scattering pair passes down the ladder of Landau levels, and $n + \Delta N$ - the number of the Landau level from which the second electron passes up the ladder of Landau levels.

$\Delta n = 1, 2, \dots$ is the absolute value of the change of the Landau level number of an individual electron of the scattering pair. As can be seen from (37), the transition of an electron down the ladder of Landau levels with a decrease in the level number is always accompanied by the transition of another electron up the ladder of Landau levels with an increase of the number by the same value. In this case, the first electron decreases its energy by the value of $\hbar\omega_c\Delta n$, while the second electron increases its energy by the same value. In the following, we will use the concept of transferred energy E_{trans} in the electron-electron scattering event. We will define it as the value by which the energy of one electron increases (the energy of the other electron decreases by the same value). In the case of intrasubband scattering $E_{trans} = \hbar\omega_c\Delta n$, Δn is the transferred energy expressed in Landau energy units.

The value ΔN is the difference between the initial Landau level numbers of two electrons before scattering – $\Delta N = n_i - n_j$, n_i is the Landau level number of the electron, which passes up the ladder of Landau levels as a result of scattering, and n_j - the number of the initial Landau level of the second electron in the interacting pair. Accordingly, the difference in the energy of the first and second electrons before scattering is equal to $\Delta E_{init} = |E_i - E_j| = \hbar\omega_c|\Delta N|$. In other words, $|\Delta N|$ is a distance in the energy space

between the electrons of the interacting pair in their initial state (the distance on the ladder of Landau levels).

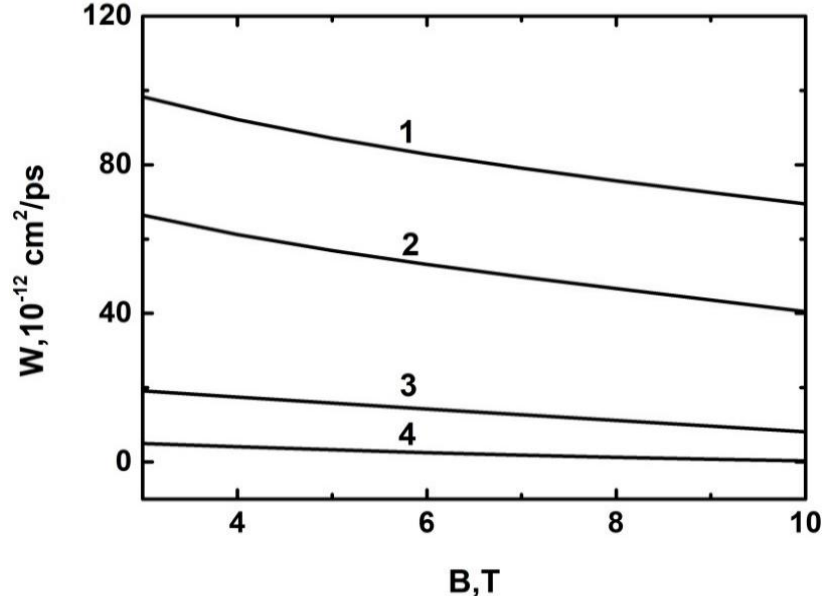


Figure 3: Dependence of the electron-electron scattering matrix elements $W \begin{pmatrix} i & j \\ f & g \end{pmatrix}$ on the magnetic field strength. 1 – $i=j=(1,3)$, $f=(1,2)$, $g=(1,4)$; 2 – $i=(1,1)$, $j=(1,2)$, $f=(1,0)$, $g=(1,3)$; 3 – $i=j=(1,3)$, $f=(1,1)$, $g=(1,5)$; 4 – $i=j=(1,3)$, $f=(1,0)$, $g=(1,6)$.

If $\Delta N=0$, the formula (38) takes the form

$$\{n \rightarrow n - \Delta n \text{ \& } n \rightarrow n + \Delta n\}. \quad (39)$$

and, as can be easily seen, describes transitions when, before scattering, both electrons are at the same Landau level n . Examples of transitions with $\Delta N=0$ are shown graphically in Figure 4a.

If $\Delta N \neq 0$ formula (38) describes transitions when electrons scatter from different Landau levels. In this case, ΔN can be either positive or negative.

When $\Delta N > 0$, an electron of a scattering pair that passes to a higher Landau level is, before scattering, at a Landau level with a number greater than n and, therefore, has a higher energy. As a result of scattering, the difference in the numbers of Landau levels and, accordingly, in the energy of electrons increases (electrons move away from each other along the ladder of Landau levels). Figure 4b shows the scheme of such transitions.

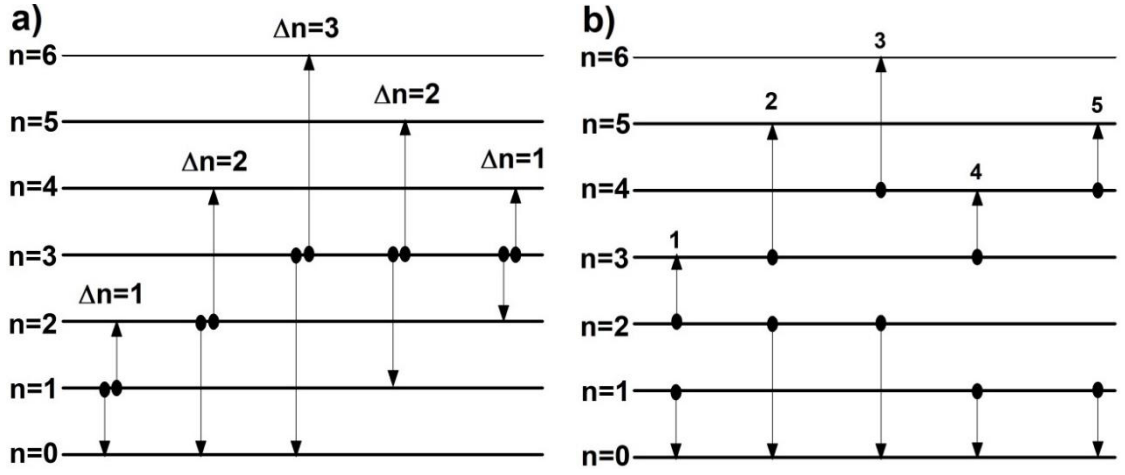


Figure 4. Schematic of intrasubband transitions (a) with $\Delta N = 0$; (b) with $\Delta N > 0$:

- 1 - $(\Delta N = 1, \Delta n = 1)$, 2 - $(\Delta N = 1, \Delta n = 2)$, 3 - $(\Delta N = 2, \Delta n = 2)$, 4 - $(\Delta N = 2, \Delta n = 1)$,
5 - $(\Delta N = 3, \Delta n = 1)$

At $\Delta N < 0$, on the contrary, the electron of the scattering pair passing to the higher level is initially lower on the ladder of Landau levels than the electron passing down the ladder. Thus, in this case, the electrons transit toward each other along the ladder of Landau levels. Among such transitions, we can distinguish transitions with $|\Delta N| \geq 2\Delta n$ (Fig. 5a) and transitions with $|\Delta N| < 2\Delta n$ with (Fig. 5b). In the first case, the electron in the interacting pair, which has a higher energy in the initial state, also has a higher energy after scattering. In the second case, this electron has a lower energy after scattering than the second electron of the pair (crossing transitions take place).

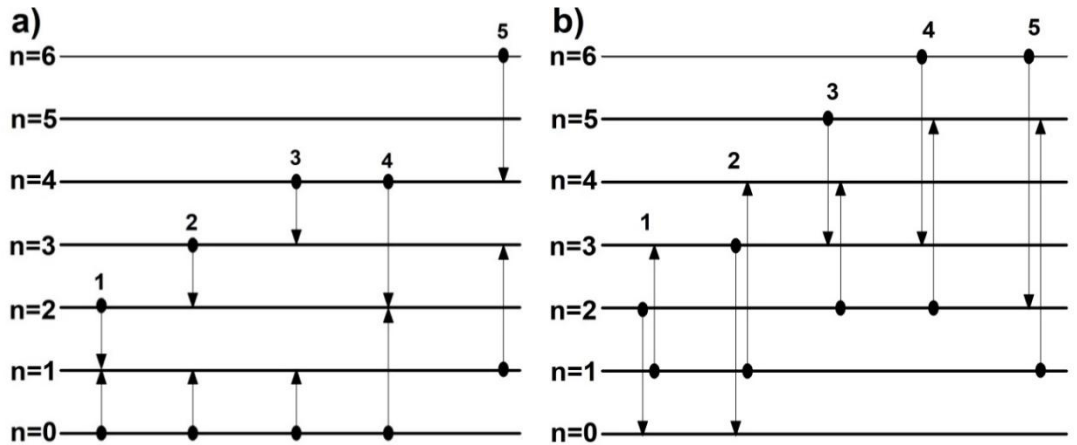


Figure 5. Scheme of intrasubband transitions with $\Delta N < 0$: a) $|\Delta N| \geq 2\Delta n$:

- 1 - $(\Delta N = -2, \Delta n = 1)$, 2 - $(\Delta N = -3, \Delta n = 1)$, 3 - $(\Delta N = -4, \Delta n = 1)$,
4 - $(\Delta N = -4, \Delta n = 2)$, 5 - $(\Delta N = -5, \Delta n = 2)$; b) $|\Delta N| < 2\Delta n$: 1 - $(\Delta N = -1, \Delta n = 2)$,
2 - $(\Delta N = -2, \Delta n = 3)$, 3 - $(\Delta N = -3, \Delta n = 2)$, 4 - $(\Delta N = -4, \Delta n = 3)$,
5 - $(\Delta N = -5, \Delta n = 4)$

In this work, we have considered various combinations of n , Δn and ΔN for quantum wells with different widths, thus studying all possible types of intrasubband transitions. As a result, the following trends of the behaviour of the elements of the electron-electron scattering rate matrix have been established.

First, the rates of intrasubband transitions decrease rapidly with increasing Δn and, consequently, with the energy E_{trans} transferred to one electron. The above is illustrated by Figure 6, which shows a typical dependence of the transition rate on Δn and, respectively, on the E_{trans} .

The tendency of decreasing matrix elements between stationary states as the energy difference between them increases is quite common in quantum systems. It is because as a state's energy increases, the number of zeros of the wave-function increases, which leads to a decrease in the integral defining the matrix element. In particular, this circumstance is the basis of truncated basis methods, in which not the full exact basis with an infinite number of states is used, but only a finite number of states corresponding to levels falling in a finite energy range. In our case, the wave-function of the one-electron state (ν, n) is the product of the wave function of the ν -th subband by the wave function of the n th energy level of the linear harmonic oscillator, which has n zeros. At the intrasubband transition from level n to level $n \pm \Delta n$, the subband wave function does not change, but the number of zeros in the oscillator wave function changes by Δn , which leads to a change by Δn the number of zeros of the first electron wave-function in the matrix element integral. Similarly, the number of zeros in the second electron wave-function also changes by Δn . As a result, the matrix element of the transition $\{n \rightarrow n - \Delta n \& n + \Delta N \rightarrow n + \Delta N + \Delta n\}$ decreases with increasing Δn , and, accordingly, the transition rate decreases. Moreover, the difference between the transition rates with Δn and $\Delta n + 1$ decreases with increasing Δn . The explanation is that the more zeros the wave-function has, the weaker it changes when one zero is added.

We emphasise that in the considered system, the transition rate decreases relatively fast—the rates of transitions with $\Delta n = 1$ are several times higher than those of transitions with $\Delta n > 1$.

The above reasoning also explains another discovered property of intrasubband scattering processes - their rates increase with deceleration (the second derivative is

negative) as n increases. As an illustration, Figure 7 shows the dependences of the $\{n \rightarrow n-1 \text{ \& } n + \Delta N \rightarrow n + \Delta N + 1\}$ transition rates on n while Δn and Δn are fixed. The higher the number of zeros the wave function has, the less it changes when adding another zero.

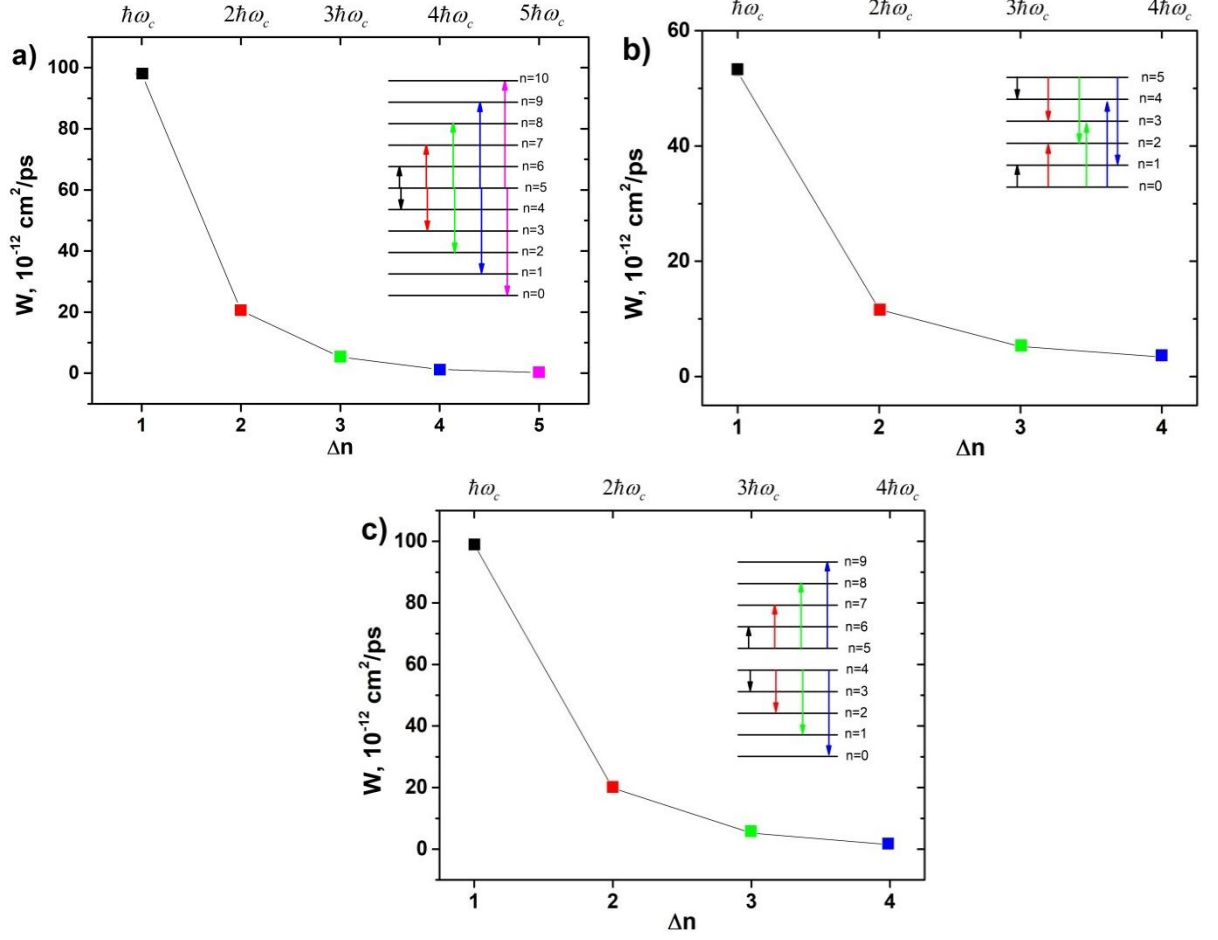


Figure. 6. Dependence of the intrasubband transition rate on the change of the Landau level number of the electron at the transition Δn (bottom axis) and, accordingly, on the transferred energy E_{trans} (top axis). Magnetic field strength $B = 3.5 \text{ T}$. a) $n = 5, \Delta N = 0$; b) $n = 5, \Delta N = -5$; c) $n = 4, \Delta N = 1$. The inserts show the schemes of transitions. The colour of the arrows indicating the transition coincides with the colour of the point on the graph.

The dependence of the electron-electron scattering rate on the difference in the Landau level numbers of the interacting electrons ΔN and, accordingly, the difference in their energy before scattering (the difference in the energies of the interacting electrons in the initial state of the corresponding transitions) was somewhat unexpected, at first glance.

With increasing $|\Delta N|$ (the difference in the energy of the electrons before scattering), the electron-electron scattering rate decreases. However, this dependence is relatively weak, so the rates of transitions in the initial states of which the electrons are at levels rather far apart on the Landau level ladder are close to the rates of transitions in which the interacting electrons are initially at the same Landau level.

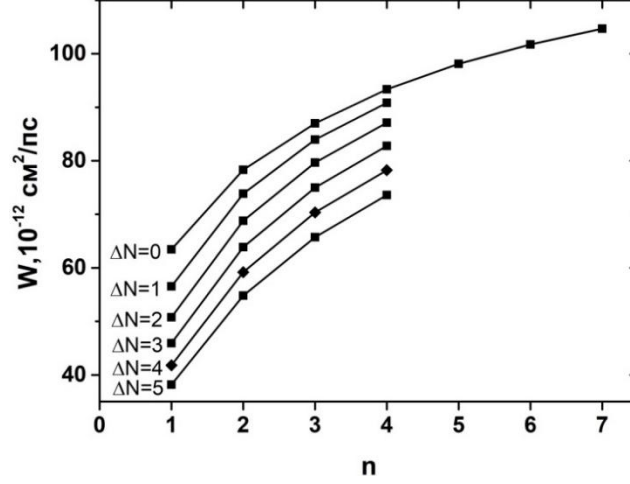


Figure 7. Dependence of the intrasubband electron-electron scattering rate on n at fixed values of Δn and ΔN . Different curves correspond to different values of ΔN . For all transitions $\Delta n = 1$. Magnetic field $B = 3.5$ T.

As an illustration, Figure 8 shows a typical intrasubband electron-electron scattering rate dependence on ΔN . The different curves correspond to transitions $\{n \rightarrow n-1 \text{ \& } n + \Delta N \rightarrow n + \Delta N + 1\}$ with varying values of n . For all transitions shown in Figure 8 $\Delta n = 1$. The scattering rate is seen to weakly decrease with increasing ΔN .

One can explain this behaviour in the following way. The difference between the wave-functions of the initial states of the electrons of the scattering pair increases with increasing ΔN , which leads to a decrease in the transition matrix element. However, in the matrix element integral (20), the variables \mathbf{r}_1 at the wave functions of the initial and final states of the first electron differ from the variables \mathbf{r}_2 at the wave functions of the second electron of the scattering pair (the variables at the wave functions of the first and second electron are independent). Therefore, the difference in the wave functions of different electrons (i.e., ΔN) has a much weaker effect on the scattering rate than that of a single electron (i.e., Δn).

In the curves presented in Figure 8, the initial and final Landau levels of one electron are fixed, while for the second electron, the number of the level from which it

moves up the ladder of Landau levels is increasing. Following our "concept of zeros", this should increase the transition rate and partially compensate for the decrease in the matrix element caused by the increase in ΔN .

Therefore, one would expect that in a transition sequence where the initial and final Landau levels of one electron are fixed and the second electron moves down the ladder of Landau levels, the decrease in the transition matrix element with ΔN could be pretty significant.

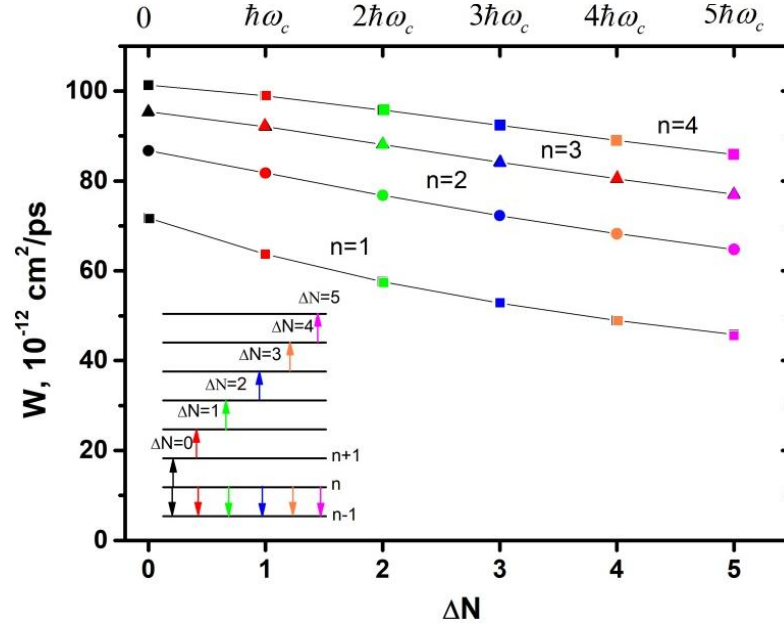


Figure 8. Dependence of the intrasubband electron-electron scattering rate on the distance between the Landau levels from which the transition occurs (lower axis). The corresponding energy difference of the electrons of the interacting pair in the initial transition state is plotted on the upper axis. Magnetic field $B=3.5$ T.

However, the analysis has shown that this is not the case - for all transition sequences, the scattering rate dependence on ΔN is weak.

As an illustration, Figure 9 shows the dependence of the transition rate on ΔN for the transition sequence when the initial and final Landau levels of the electron going up the ladder of Landau levels are fixed (the electron moves from level $n=4$ to level $n=5$) and the initial Landau level of the second electron of the scattering pair moves down the ladder of Landau levels. (the electron moves from level n to $n-1$, where n decreases from 4 to 1 while ΔN increasing from 0 to 3). In this case, according to the "concept of zeros", the decrease of n and the increase of ΔN work both towards reducing the transition matrix element. As can be seen, the dependence on ΔN is slightly increased compared to the situation presented in Figure 8. Nevertheless, this dependence is relatively weak.

The relatively large value of the scattering rate for $\Delta N \neq 0$ transitions is of great importance for the physical picture of relaxation in the Landau level system because of its specific mechanism. This mechanism consists of electron-electron scattering processes delivering electrons to the optical phonon level from the underlying Landau levels. Having reached Landau levels lying above or near the optical phonon energy, the electrons transfer energy to the optical vibrations of the crystal lattice in electron-phonon scattering processes [12].

The process of energy relaxation can be understood through two parallel mechanisms. The first involves the redistribution of electrons among Landau levels due to electron-electron scattering. This creates a quasi-Boltzmann distribution with an effective temperature that is significantly higher than that of the crystal lattice. The second mechanism is the promotion of electrons to higher Landau levels, also caused by electron-electron scattering. This is followed by the emission of optical phonons, which helps to transfer the excitation energy of the electron subsystem to the crystal lattice.

Electron-electron scattering processes with $\Delta N \neq 0$ lead to intense transitions, as electrons at the upper levels interact with those in the highly populated lower Landau levels. This interaction significantly accelerates the thermalization of the electron subsystem [14]. Simultaneously, these transitions "pull away" electrons from the upper Landau levels, which weakens the flow of electrons to the optical phonon level. As a result, there is a strong dependence of the relaxation time on the population of the ground Landau level [14].

To emphasize the significance of the $\Delta N \neq 0$ transitions in relaxation processes, we present an example in Figure 10 that illustrates the time dependence of the excitation energy of the electron subsystem. This data is calculated with and without considering the $\Delta N \neq 0$ transitions. The comparison of these curves shows that neglecting the $\Delta N \neq 0$ transitions leads to a substantial slowdown in energy relaxation, causing the relaxation time to increase by more than an order of magnitude — rising from 0.16 ns to 2.44 ns.

We also note that while the rate of transitions with $\Delta n > 1$ is several times lower than the rate of transitions with $\Delta n = 1$, the nonlinear nature of electron-electron scattering causes transitions with larger Δn to significantly influence the quantitative aspects of the relaxation kinetics. This effect is illustrated in the inset of Figure 10, which shows the time evolution of the excitation energy of the system. One graph considers all

Δn transitions, while the other only includes those with $\Delta n = 1$. The results demonstrate that accounting for transitions with $\Delta n > 1$ leads to a noticeable decrease—approximately 25%—in the energy relaxation time.

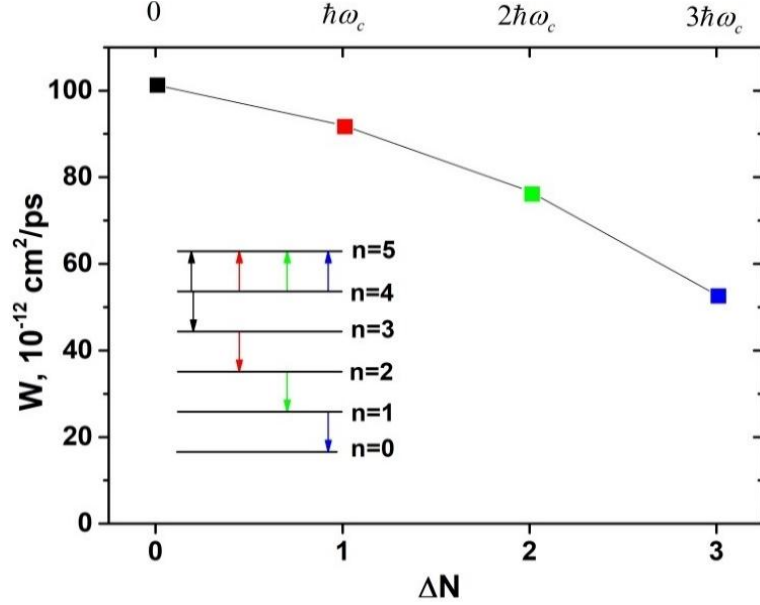


Figure 9. Scattering rates for transitions $\{(1, 4) \rightarrow (1, 5) \text{ \& } (1, 4 - \Delta N) \rightarrow (1, 4 - \Delta N - 1)\}$ as a function of ΔN .

We emphasize that if only transitions with the highest rates (transitions with $\Delta N = 0$ and $\Delta n = 1$) are included in the relaxation kinetics, the error in determining the relaxation time increases significantly. Specifically, the relaxation time is calculated to be 17.5 ns instead of the accurate 0.16 ns when all transitions are considered.

We also observe that for the lowest subbands, there is a relatively small decrease in the scattering rate as the quantum well width increases (see Fig. 11). This phenomenon occurs for a reason similar to the reduction in exciton binding energy within a quantum well as the well width increases [29]. As the width of the well grows, the localization length of the wave function also increases, causing the probability density of the electron's position to become more uniformly distributed over this length. Consequently, the average distance between electrons increases, which results in a decreased scattering probability.

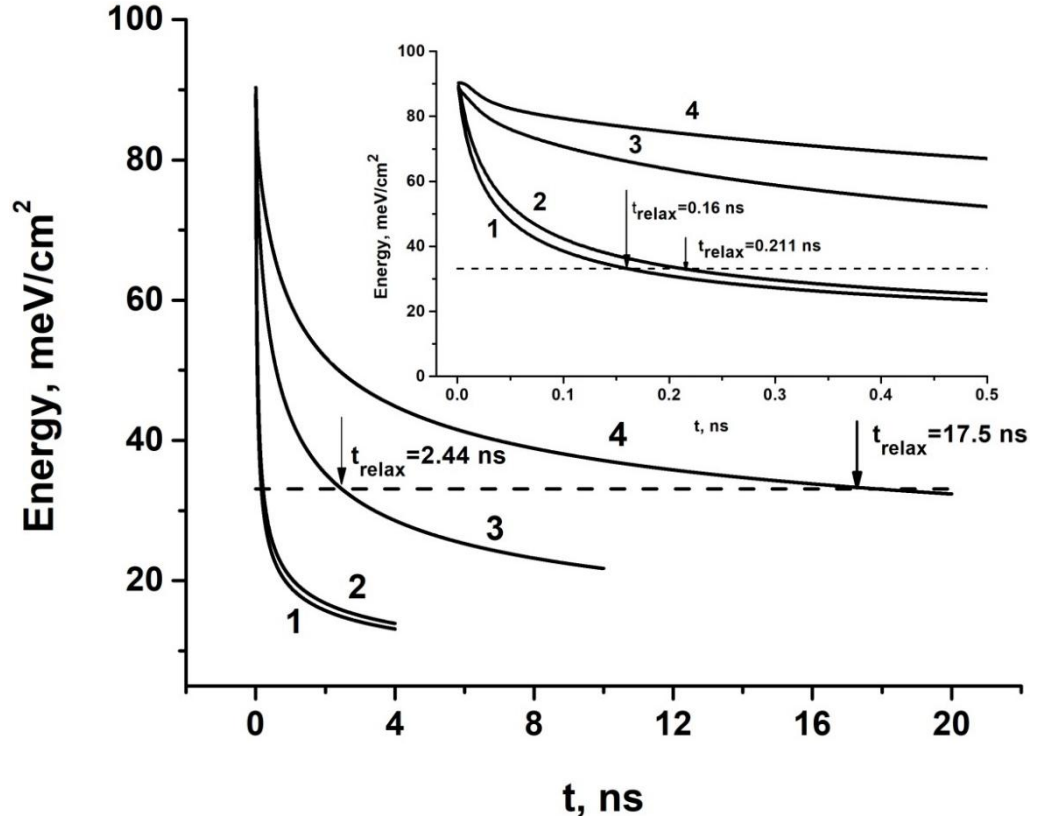


Figure 10. Dependence of the excitation energy of the electronic subsystem on time. Magnetic field $B=3.5$ T (at this value, the Landau level (1,6) is close to the optical phonon energy). Crystal lattice temperature is 4.2 K. Electron density in quantum well is $1.5 \cdot 10^{10} \text{ cm}^{-2}$. Nonequilibrium is created by the instantaneous excitation of $5 \cdot 10^9 \text{ cm}^{-2}$ electrons to the Landau (1,3) level. 1 –all electron-electron scattering processes from Landau levels lying below the optical phonon energy were included; 2 – only scattering transitions with $\Delta n=1$ were considered; 3 –only transitions with $\Delta N=0$ were considered (but with all possible Δn); 4 – only transitions with $\Delta N=0$ and $\Delta n=1$ were considered. The horizontal dashed line shows the value of the excitation energy, which is e times smaller than the initial value.

In the case of multiple subbands, a special type of transition occurs when each electron in an interacting pair remains in the same subband after scattering as it was initially, but the electrons belong to different subbands. This type of transition is referred to as intrasubband transitions of type II and is schematically shown in Fig. 2e. Each electron's transition is intrasubband. Therefore, the resonance condition for the transition is still described by expression (37) and holds for any value of the magnetic field. As a result, the magnetic field dependence of the transition rate for type II is similar to that of type I transitions—the transition rate gradually decreases as the strength of the magnetic field increases (see Fig. 12). In this scenario, the change in the Landau level number for one electron during the electron-electron scattering event is equal in magnitude but

opposite in sign to the change in the Landau level number for the other electron. Thus, the same kinds of transitions occur as for type I, with the only distinction being that the electrons traverse the ladder of Landau levels in different subbands. The complete set of all intrasubband transitions of type II, for which the law of energy conservation is satisfied, can be described by the formulas.

$$\{(v_i, n_i) \rightarrow (v_i, n_i - \Delta n) \& (v_j, n_j) \rightarrow (v_j, n_j + \Delta n)\} \quad (39)$$

and

$$\{(v_i, n_i) \rightarrow (v_i, n_i + \Delta n) \& (v_j, n_j) \rightarrow (v_j, n_j - \Delta n)\}, \quad (40)$$

Here, as well as in type I, the energy E_{trans} transferred to the electron is proportional to the number of levels through which the electron "jumps".

At transitions of type II, there is a similar dependence on the energy E_{trans} transferred to the electron - the rate of transitions of type II strongly decreases as transferred energy E_{trans} increases (Fig. 13). The explanation of this trend is the same as in the case of intrasubband transitions.

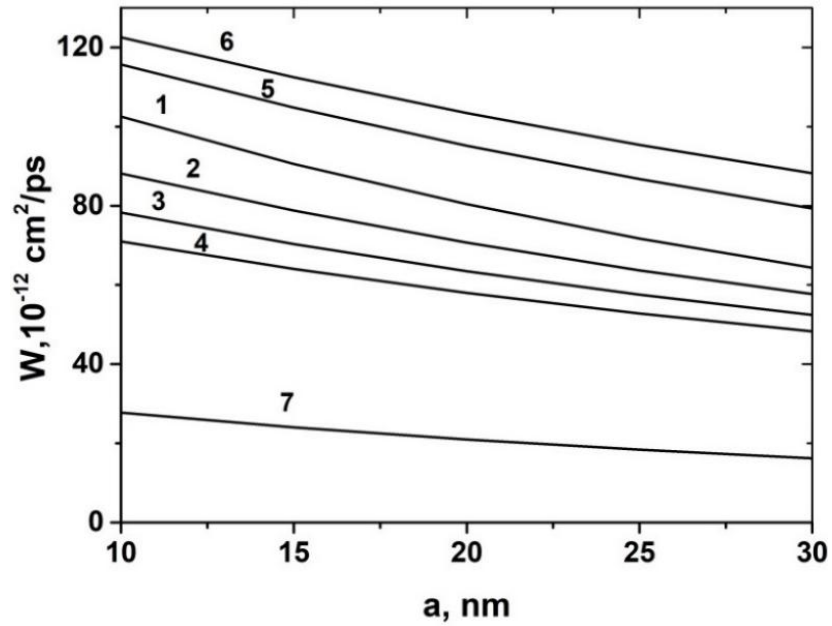


Figure 11. Dependence of the scattering rate on the quantum well width. 1- ($n=1$, $\Delta N=0$, $\Delta n=1$); 2- ($n=1$, $\Delta N=1$, $\Delta n=1$); 3- ($n=1$, $\Delta N=2$, $\Delta n=1$); 4- ($n=1$, $\Delta N=3$, $\Delta n=1$); 5 – ($n=2$, $\Delta N=0$, $\Delta n=1$); 6 – ($n=3$, $\Delta N=0$, $\Delta n=1$); 7 – ($n=3$, $\Delta N=0$, $\Delta n=2$).

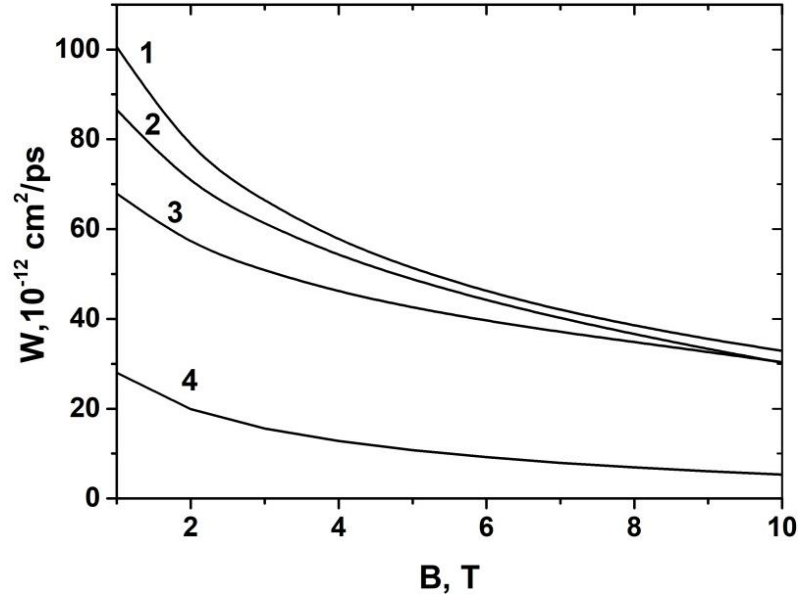


Figure 12. Dependence of the electron-electron scattering rate on the magnetic field for intrasubband transitions of type II: 1 - $\{(2,0) \rightarrow (2,1) \& (1,1) \rightarrow (1,0)\}$; 2 - $\{(2,1) \rightarrow (2,2) \& (1,1) \rightarrow (1,0)\}$; 3 - $\{(2,0) \rightarrow (2,1) \& (1,4) \rightarrow (1,3)\}$; 4 - $\{(2,0) \rightarrow (2,2) \& (1,2) \rightarrow (1,0)\}$.

It's important to note that the rates of type I and type II transitions are quite close in magnitude (refer to Fig. 14). This similarity is critical for understanding how electrons relax from the Landau levels of the upper subband, which lies below the energy of optical phonon. When electrons are excited into the upper subband, type II transitions create and activate a strong relaxation channel. In this process, electrons move along the ladder of Landau levels within the upper subband and transit to the lower subband as a result of intersubband electron-phonon scattering processes [15].

Figure 15 illustrates the importance of type II transitions in the processes of intersubband relaxation. It depicts the temporal dependence of the electron subsystem energy when selectively excited to the Landau level (2,0), which is positioned below the optical phonon energy. In the first curve (curve 1), all electron-electron scattering processes from Landau levels below the optical phonon energy are taken into account. In the second curve (curve 2), intrasubband transitions of type II are disregarded. It is evident that neglecting type II transitions significantly slows down the relaxation rate, resulting in an increase in relaxation time of more than three times.

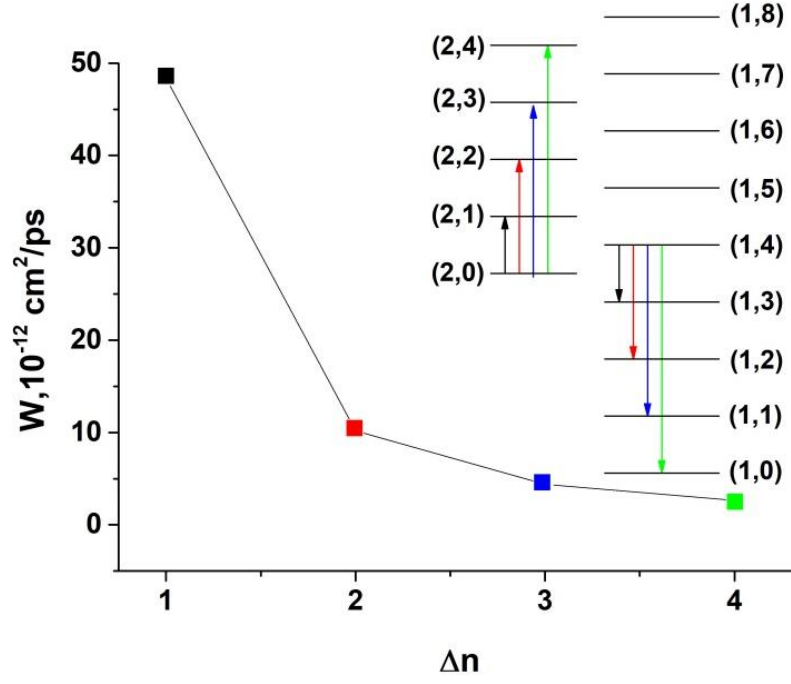


Figure 13. Dependence of the electron-electron scattering rate for type II intrasubband transitions on the change in Δn of the Landau level number of the electron at the transition. Magnetic field $B=3.5$ T.

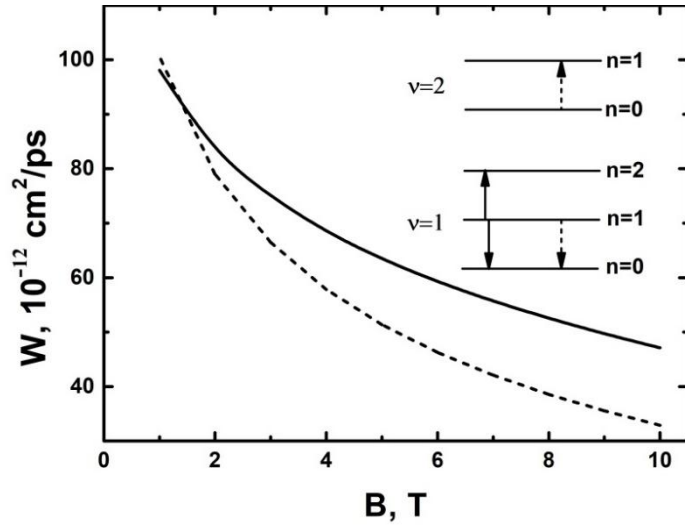


Figure 14. Dependence of the electron-electron scattering rate on the magnetic field for the intrasubband transition of type I $\{(1,1) \rightarrow (1,0) \& (1,1) \rightarrow (1,2)\}$ (solid curve) and intrasubband transition of type II $\{(1,1) \rightarrow (1,0) \& (2,0) \rightarrow (2,1)\}$ (dashed line).

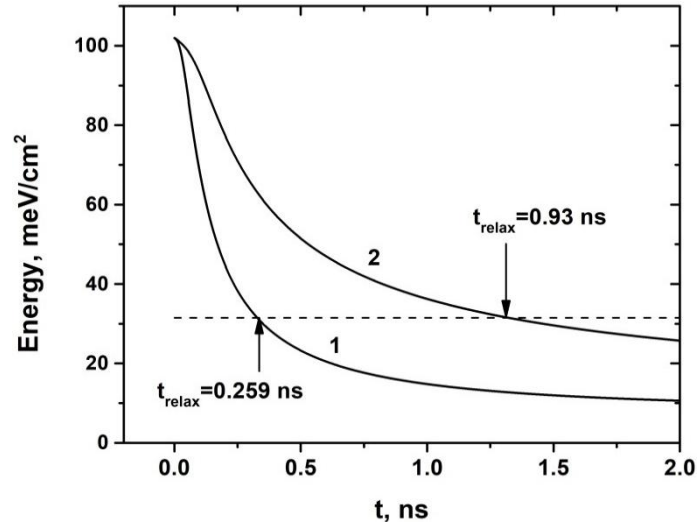


Figure 15. Time dependence of the excitation energy of the electron subsystem after its selective excitation to the Landau (2,0) level. Magnetic field $B=3.5$ T (at this value, the optical phonon level passes near the Landau level (2,3)). Temperature of the crystal lattice is 4.2 K. Concentration of electrons in the quantum well is $1.5 \cdot 10^{10} \text{ cm}^{-2}$. The nonequilibrium is created by instantaneous excitation of $5 \cdot 10^9 \text{ cm}^{-2}$ electrons to the Landau level (2,0). Curve 1 was calculated considering all transitions from Landau levels below the optical phonon energy. In calculating curve 2, intrasubband transitions of type II are neglected.

5. Inter-subband transitions

We divide the electron-electron scattering transitions between two subbands into three types.

In intersubband transitions of type I, both electrons of the interacting pair are in one subband ($\nu_i = \nu_j$) and, as a result of scattering, move to the Landau levels of the other subband ($\nu_g = \nu_f \neq \nu_i = \nu_j$). Examples of transitions of this type are shown in Fig. 2a and Fig. 2b.

In type II, we refer to transitions in which only one electron moves to the other subband while the second electron stays in the initial subband, i.e. $\nu_j \neq \nu_g$. Examples of transitions of this type are shown in Fig. 2c.

In the initial state of transitions of type III, the electrons of the interacting pair are in different subbands ($\nu_i \neq \nu_j$), and each of them transits to the Landau levels of the other subband ($\nu_f = \nu_j$ and $\nu_g = \nu_i$). Examples of transitions of this type are shown in Fig. 2d.

In contrast to intra-subband scattering, the nature of the rate dependence on the magnetic field of inter-subband transitions depends on their type.

In transitions of type I, the energy conservation law $E_{(v_i, n_i)} + E_{(v_i, n_j)} = E_{(v_f, n_f)} + E_{(v_f, n_g)}$ takes the form

$$n_f + n_g - n_i - n_j = 2 \frac{\Delta \varepsilon_{if}}{\hbar \omega_{\perp}}, \quad (41)$$

where

$$\Delta \varepsilon_{if} = \varepsilon_{v_i} - \varepsilon_{v_f} \quad (42)$$

is the inter-subband spacing.

This condition is satisfied in two cases: if $\frac{\Delta \varepsilon_{if}}{\hbar \omega_{\perp}}$ is an integer

$$\frac{\Delta \varepsilon_{if}}{\hbar \omega_{\perp}} = p, \quad (43)$$

where $p = 1, 2, 3, \dots$;

or $\frac{\Delta \varepsilon_{if}}{\hbar \omega_{\perp}}$ is a half-integer

$$\frac{\Delta \varepsilon}{\hbar \omega_{\perp}} = p + \frac{1}{2}, \quad (44)$$

where $p = 0, 1, 2, 3, \dots$

Condition (43) corresponds to the value of the magnetic field

$$B_{\perp, n} = \frac{m_w c}{\hbar e} \frac{\Delta \varepsilon_{if}}{p}, \quad (45)$$

at which the 0-th Landau level of the upper subband coincides with the p-th Landau level of the lower subband ($E_{(v_i, 0)} = E_{(v_f, p)}$). Since the system of Landau levels of a subband is equidistant and the distance between neighbouring levels is the same in each subband, the alignment with the Landau levels of the lower subband will simultaneously occur for all Landau levels of the upper subband – $E_{(v_i, n)} = E_{(v_f, p+n)}$, where $n = 0, 1, 2, \dots$ (see Fig. 16).

Therefore, at the value of the magnetic field satisfying condition (45), a large number of transitions are simultaneously in resonance. All these transitions can be described by the formula

$$\left\{ (\nu_i, n) \rightarrow (\nu_f, p + n - \delta n) \& (\nu_i, n + \Delta N) \rightarrow (\nu_f, p + n + \Delta N + \delta n) \right\}. \quad (46)$$

In this formula, n is the number of the initial Landau level of the electron in the upper subband whose energy decreases in the scattering act. The energy transferred to one electron in the scattering act is $E_{trans} = |E_f - E_i| = |E_g - E_j| = \hbar\omega_c \cdot \delta n$. The difference between the energy in the initial state of the electron that moves to the higher level and the energy of the second electron of the interacting pair is $\Delta E_{init} = \hbar\omega_c \cdot \Delta N$.

In formula (46) δn is still the energy transferred to one electron in the scattering act, expressed in units of $\hbar\omega_c$. However, δn now differs from the change in the Landau level number in the subband at the transition as for an electron whose energy decreases with scattering,

$$n_f - n_i = p - \delta n, \quad (47)$$

and for the electron whose energy increases during scattering,

$$n_g - n_j = p + \delta n. \quad (48)$$

Depending on the sign of the difference ΔN between the numbers of the initial Landau levels, we have different kinds (subtypes) of type I inter-subband transitions.

In case of $\Delta N = 0$ formula (46) describes transitions, when both electrons are at the same Landau level (ν_i, n) in the initial state. In this case $\Delta n \leq p + n$.

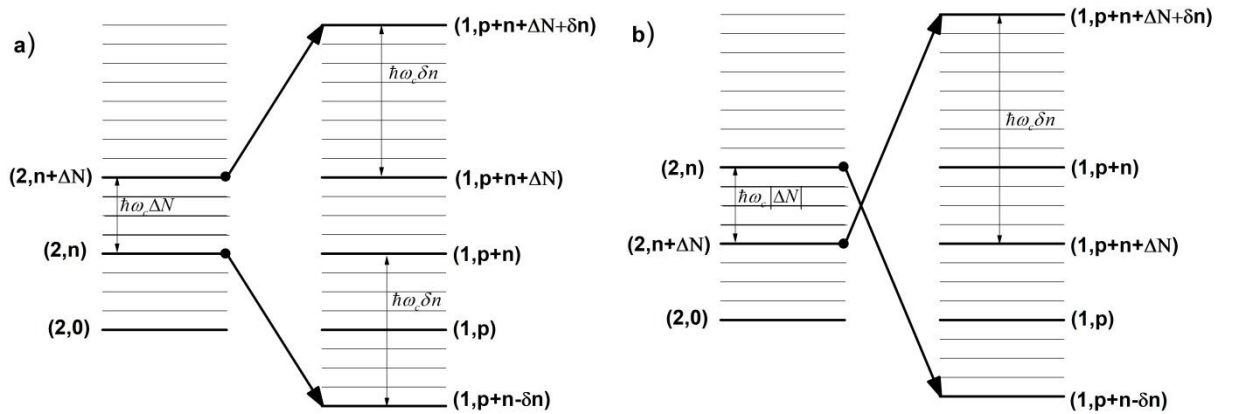


Figure 16. Scheme of intersubband transitions of type I in the case when the upper subband's Landau levels coincide with the lower subband's Landau levels: a) at $\Delta N \geq 0$; b) at $\Delta N < 0$.

The value $\Delta N \neq 0$ corresponds to the transitions in which the electrons of the interacting pair are initially at different Landau levels - the electron whose energy

decreases in a scattering event is at the level (ν_i, n) , and the second electron is at the level $(\nu_i, n + \Delta N)$.

An example of transitions with $\Delta N > 0$ is shown in Figure 16a. In this case $\Delta n \leq p + n$. An example of transitions with $\Delta N < 0$ is shown in Figure 16b. In this case $\Delta N \geq -n$.

Condition (44) corresponds to the value of the magnetic field

$$B_{\perp, n} = \frac{m_w c}{\hbar e} \frac{\Delta \mathcal{E}_{if}}{p + \frac{1}{2}}, \quad (49)$$

at which the 0-th Landau level of the upper subband lies precisely in the middle between the p-th and (p+1)-th Landau levels of the lower subband ($E_{(\nu_i, 0)} = (E_{(\nu_f, p)} + E_{(\nu_f, p+1)}) / 2$).

Correspondingly, all higher levels of the upper subband lie exactly midway between the neighbouring Landau levels of the lower subband – $E_{(\nu_i, n)} = (E_{(\nu_f, p+n)} + E_{(\nu_f, p+n+1)}) / 2$,

where $n=0, 1, 2, \dots$ (see Fig. 17). Thus, the resonance condition is simultaneously satisfied for a set of transitions. All this set of transitions can be described by the formula

$$\left\{ (\nu_i, n) \rightarrow \left(\nu_f, p + n + \frac{1}{2} - \delta n \right) \& (\nu_i, n + \Delta N) \rightarrow \left(\nu_f, p + n + \Delta N + \frac{1}{2} + \delta n \right) \right\}. \quad (50)$$

Also, as before, δn is the energy transferred to one electron expressed in units of $\hbar \omega_c$, i.e. $E_{trans} = |E_f - E_i| = |E_g - E_j| = \hbar \omega_c \cdot \delta n$, but now δn takes half-integer positive values, less than or equal to $p + n + 1/2$. At $\delta n = 1/2$, the electrons pass to the nearest Landau levels of the lower subband, at $\delta n = 3/2$, to the levels of the lower subband following the nearest ones, etc. In formula (50) ΔN can take integer values greater than $-\delta n$. Schemes of transitions with $\Delta N \geq 0$ and $\Delta N < 0$ are shown in Figures 17a and 17b, respectively. The change of the Landau level number in the subband for an electron whose energy decreases as a result of the interaction is

$$n_f - n_i = p - \left(\delta n - \frac{1}{2} \right), \quad (51)$$

and for the electron whose energy increases

$$n_g - n_j = p + \left(\delta n + \frac{1}{2} \right). \quad (52)$$

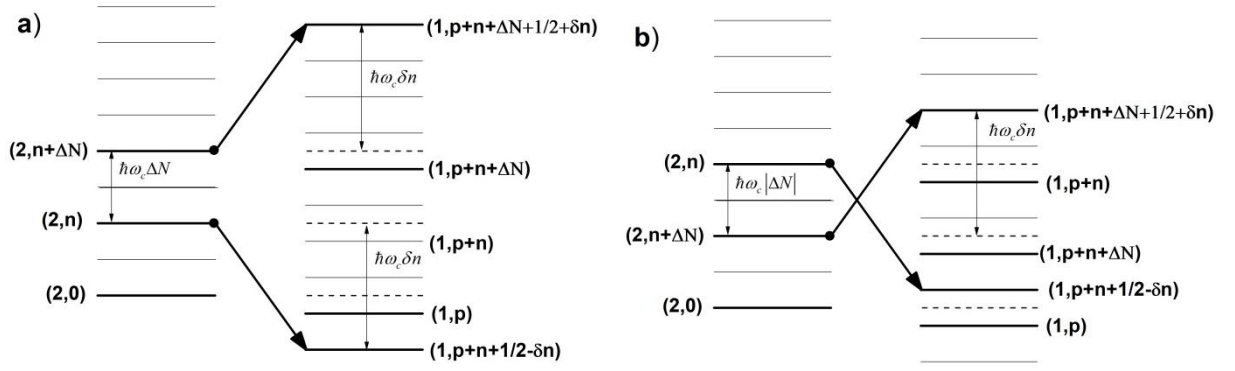


Figure 17. The scheme of intersubband transitions of type I when the Landau levels of the upper subband are in the middle between the Landau levels of the lower subband a) for $\Delta N > 0$; b) for $\Delta N < 0$.

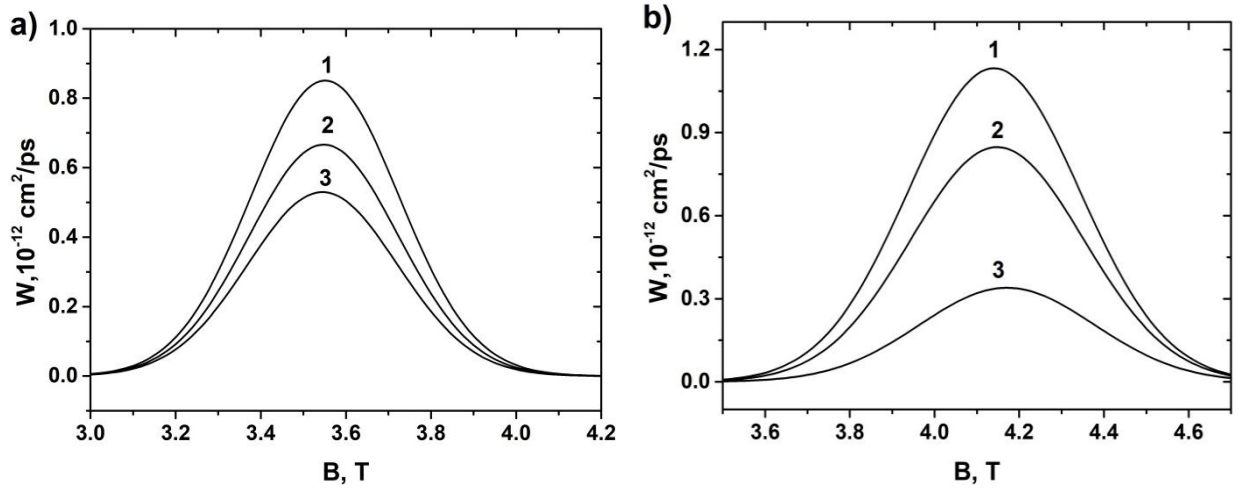


Figure 18. Dependence of the electron-electron scattering rate on the magnetic field for transitions of the type I. a) 1 - $\{(2,0) \rightarrow (1,3) \text{ \& } (2,0) \rightarrow (1,4)\}$, 2- $\{(2,0) \rightarrow (1,3) \text{ \& } (2,1) \rightarrow (1,5)\}$, 3- $\{(2,0) \rightarrow (1,3) \text{ \& } (2,2) \rightarrow (1,6)\}$.
 б) 1- $\{(2,0) \rightarrow (1,3) \text{ \& } (2,0) \rightarrow (1,3)\}$, 2- $\{(2,0) \rightarrow (1,2) \text{ \& } (2,0) \rightarrow (1,4)\}$, 3 - $\{(2,0) \rightarrow (1,1) \text{ \& } (2,0) \rightarrow (1,5)\}$.

For each type I inter-subband transition, the energy conservation law is satisfied at only one specific value of the magnetic field. This value is determined either by the expression in (45) or by the one in (49). Given that Landau levels have a finite width, the dependence of the type I inter-subband transition rate on the magnetic field manifests as a resonance peak (see Fig. 18).

A comparison with intra-subband scattering rates indicates that the rates of type I inter-subband scattering—even at resonance—are significantly lower (by about two orders of magnitude) than those for both type I and type II intra-subband scattering. However, type I inter-subband transitions facilitate the transfer of electrons from the

upper subband to the lower subband, making them an important channel for inter-subband relaxation.

For type I inter-subband transitions, it is interesting to ask whether it is possible to make a simple separation of matrix elements by their magnitude, similar to how we do for intra-subband transitions by the magnitude of energy transferred by scattering to one electron. At first glance, it would seem that for inter-subband transitions of type I, there should be a dependence of the transition rate on E_{trans} , similar to intra-subband transitions – the rate of inter-subband transitions of type I should decrease with an increase in E_{trans} . However, the scattering rate matrix analysis has revealed that this is not the case at all.

Figure 19 shows the dependencies of the rate of inter-subband transitions of type I on the transferred energy. In each of the transitions presented, the initial states of the electrons of the interacting pair are fixed (n and ΔN are their own for each figure), and the final states change as the energy (number δn) transferred to one electron in the scattering act increases, which is plotted on the abscissa axis. For inter-subband transitions, there is no such clear dependence of the scattering rate on the transferred energy as in the case of intrasubband transitions. In the case when both electrons scatter from the (2,0) level, the scattering rate decreases rather rapidly with the transferred energy (Fig. 19a). At the same time, when both electrons scatter from different Landau levels, the rates of the first few transitions can be close in magnitude (Fig. 19b), and even exceed the transition with minimal change in electron energy (Fig. 19c). A rather complex non-monotonic dependence on the transferred energy is also possible (Fig. 19d).

The behaviour of the scattering rate for the different types of transitions with a change in the transferred energy can be explained as follows.

In resonance, the transition rate is determined not directly by the change in electron energy, but rather by the difference in the wave function (14) of each electron before and after scattering. Since the structure potential and, consequently, the subband energy levels ε_ν and wave functions $\varphi_\nu(z)$ are fixed, the difference in the wave functions of the initial and final states of a transition $\{(i_i, n_i) \rightarrow (\nu_f, n_f) \& (\nu_j, n_j) \rightarrow (\nu_g, n_g)\}$ of this type is determined by the difference in the numbers of the Landau levels $\Delta n_1 = |n_f - n_i|$ and $\Delta n_2 = |n_g - n_j|$, in the subbands to which these levels belong. The smaller this difference

is, the closer the wave functions of the initial and final states are. In the case of $\Delta n_\alpha = 0$ the difference of the wave functions of the initial and final states of the α -th electron of the pair is minimal – these wave functions differ only by the subband component.

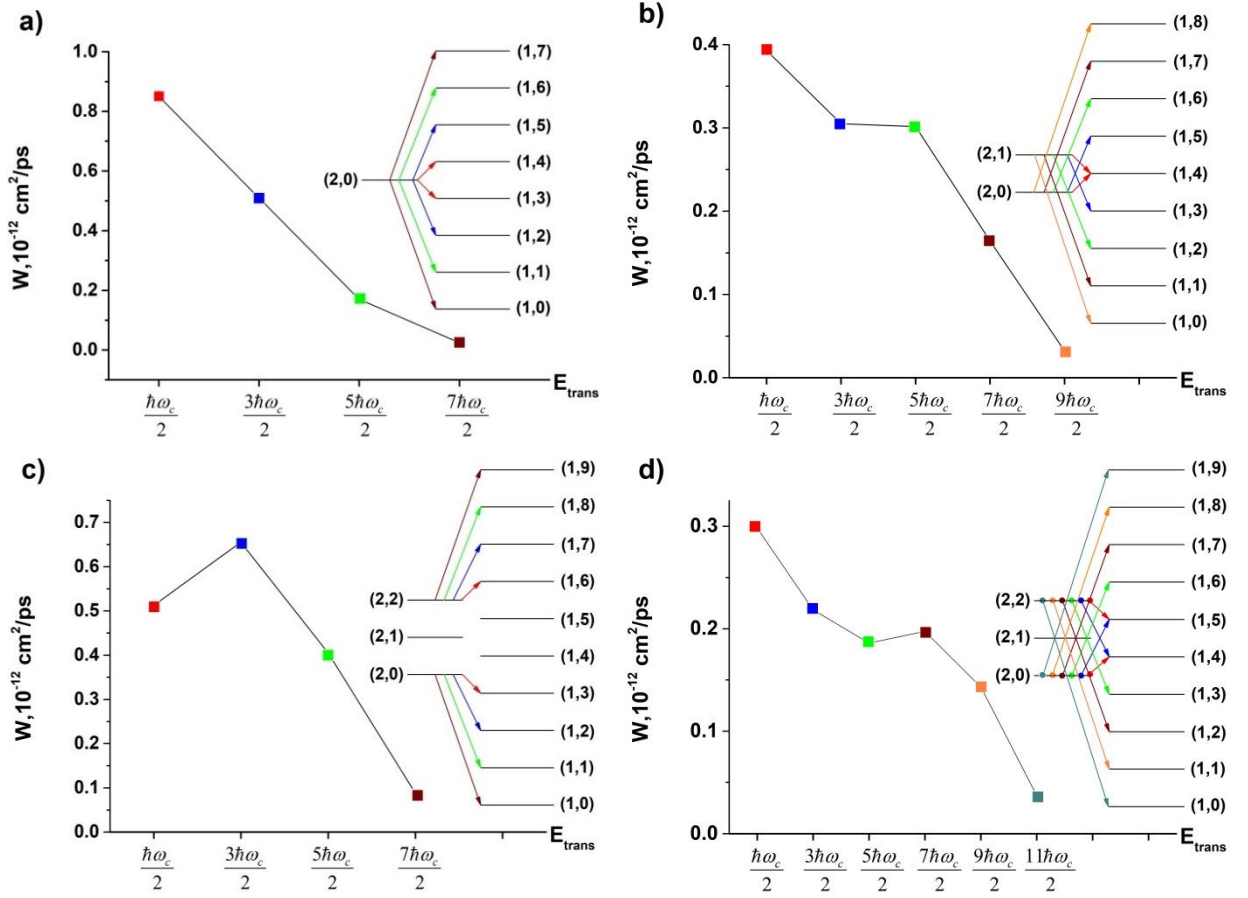


Figure 19. Dependence of the rate of type I intersubband transitions on the transferred energy E_{trans} . The magnetic field $B=3.5$ T corresponds to the situation when the Landau level (2,0) lies in the middle between the Landau levels (1,3) и (1,4).

In the case of intrasubband transitions of type I $\Delta n_1 = \Delta n_2 = \Delta n$, and the transferred energy $E_{trans} = \hbar\omega_c \cdot \Delta n$. Therefore, with the increase of E_{trans} , that is Δn , the difference between the wave functions of the initial and final states of each electron of the interacting pair increases, and, as a consequence, the transition rate decreases. This explains the observed monotonic dependence of the intrasubband transition rates on E_{trans} . The aforementioned reason also clarifies why the difference between the rates decreases with increasing Δn . This occurs because the more zeros the wave function has, the smaller the difference becomes when an additional zero is added.

In the case of inter-subband transitions of type I $\Delta n_1 \neq \Delta n_2$. This can be clearly seen in the diagrams of transitions shown in Figure 19 as insets. For example, for the transition

$\{(2,0) \rightarrow (1,3) \& (2,0) \rightarrow (1,4)\}$ the Landau level number change for one electron is $\Delta n_1 = |3-0| = 3$, and for the other is $\Delta n_2 = |4-0| = 4$. For inter-subband transitions of type I we have introduced a number δn so that $E_{trans} = \hbar \omega_c \cdot \delta n$. The value δn gives us the number of Landau levels through which the electron "jumps" at scattering (see the schematics in Figs. 16 and 17). However, since the subbands are shifted relative to each other, Δn_1 and Δn_2 does not coincide with this number of levels. The relationship of Δn_1 and Δn_2 to δn is described by expressions (47) and (48) in the case of strict coincidence of the upper and lower subband levels. For resonance, when the levels of the upper subband are positioned midway between the Landau levels of the lower subband, expressions (51) and (52) apply. From these expressions, as well as the transition diagrams shown in the insets of Figures 19, it is evident that as the transferred energy E_{trans} and δn increases, the difference in the Landau level numbers for one electron also increases, which contributes to a decrease in the transition rate. Meanwhile, for the second electron in the scattering pair, this difference initially decreases, which serves to increase the transition rate. Once the value reaches zero at $\delta n = p$ or $\delta n - \frac{1}{2} = p$, it starts to increase, acting together with the first electron in the direction of decreasing the matrix element. This increase occurs in conjunction with the first electron, and both influence the matrix element in a direction that reduces its value. Therefore, we observe that at $\delta n \leq p$ the electrons in the scattering pair behave oppositely regarding their impact on the transition rate as the value δn increases. This leads to a complex relationship between the inter-subband transition rate of type I and E_{trans} .

In the case of type III inter-subband transitions, the dependence on E_{trans} behaves similarly, though it may be more pronounced. For instance, in type III transitions, it is possible for both Δn_1 and Δn_2 to decrease simultaneously as the transferred energy E_{trans} increases, while the transition rate significantly and consistently rises with increasing E_{trans} . This scenario is illustrated in Figure 20a, where it is evident that the scattering rate increases almost by an order of magnitude with increasing E_{trans} .

However, this dependence is not a universal trend. Here, as well as in the first case, the nature of the dependence is influenced in complex ways by the initial states of the

electrons in the scattering pair. In some instances, the transition rate may decrease monotonically and rather slowly (see Fig. 20b). In other initial states of the electrons, the situation may be different: the rate can initially increase significantly before rapidly decreasing (see Fig. 20c).

The reason for this behavior here is the same as for the inter-subband transitions of type I. The magnitude of the transition rate is determined by Δn_1 and Δn_2 . Due to the fact that the subbands are shifted relative to each other, there is no unambiguous relationship between Δn_1 , Δn_2 and the transferred energy E_{trans} . The dependence of E_{trans} on Δn_1 and Δn_2 differs for different initial states. At the same time Δn_1 and Δn_2 may not coincide and can change up or down with increasing E_{trans} .

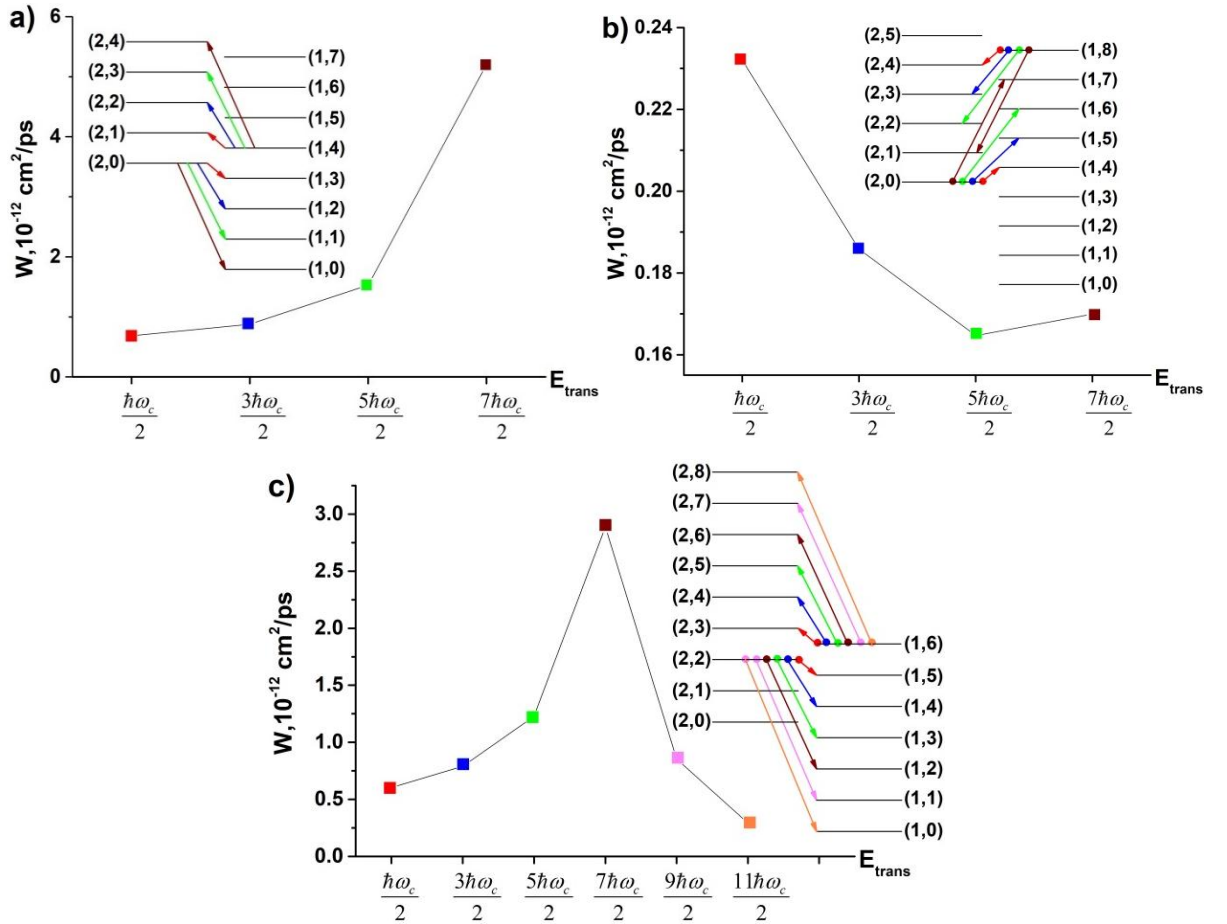


Figure 20. Dependencies of type III transitions rate on transferred energy E_{trans} . Magnetic field $B=3.5 \text{ T}$.

We arrive at an important conclusion: it is not possible to assess the relative magnitude of inter-subband transition rate based solely on the transferred energy E_{trans} . Additionally, since both Δn_1 and Δn_2 differ and can change variably depending on the

initial states of the electrons, there is no explicit relationship between the transition rate and Δn_1 and Δn_2 that holds true for all transitions of a given type. As a result, it is not feasible to determine in advance which inter-subband electron-electron scattering processes are the most significant and should be considered in kinetic assessments, and which ones are less intense and can therefore be ignored. Thus, for an accurate description of the kinetics, it is essential to compute the “complete” matrix of inter-subband transition rates.

The above is illustrated in Figure 21, which depicts the time evolution of the excitation energy of the electron subsystem after its selective excitation to the Landau level (2,0), which is situated below the optical phonon energy level. Curve 1 is calculated by considering all electron-electron scattering processes occurring among electrons at Landau levels below the energy of the optical phonon. In the calculation of Curve 2, all inter-subband electron-electron scattering processes are disregarded, except for transitions $\{(2,0) \rightarrow (1,3) \& (2,0) \rightarrow (1,4)\}$ to the nearest Landau levels of electrons that are initially at the same Landau level (2,0). As demonstrated, including the complete set of inter-subband electron-electron scattering rates results in a significant acceleration of energy relaxation, reducing the relaxation time by more than 50%.

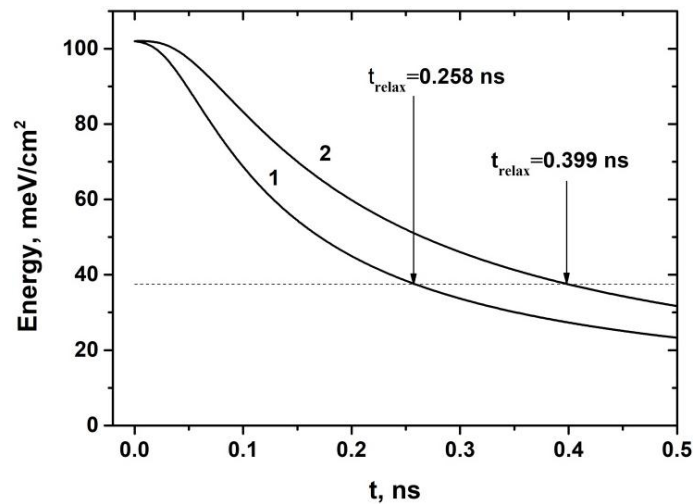


Figure 21. Dependence of the excitation energy of the electron subsystem on time calculated with "full" matrix of electron-electron scattering rates (curve 1) and neglecting all inter-subband transitions except for transitions $\{(2,0) \rightarrow (1,3) \& (2,0) \rightarrow (1,4)\}$ (curve 2). At the initial moment of time $t=0$ only two Landau levels are populated - level (2,0) with a concentration of $5 \cdot 10^9 \text{ cm}^{-2}$ and level (1,0) with a concentration of 10^{10} cm^{-2} . The magnetic field $B=3.5 \text{ T}$.

The situation with the transition rate dependence on the energy difference of the electrons before scattering $\Delta E_{init} = |E_i - E_j|$ is also not simple for similar reasons. As in the case of intrasubband transitions, the value of the matrix element is determined not by ΔE_{init} but by the difference in initial Landau level number of interacting electrons $\Delta N = n_i - n_j$, each of which is counted in its own subband.

In the case of transitions of type I, the interacting electrons are in the same subband. Accordingly, $\Delta E_{init} = \hbar\omega_c |\Delta N|$, and the rates for transitions of this type slowly decrease with ΔE_{init} (Fig. 22).

In the cases of type II intra-subband transitions and type III inter-subband transitions, the electrons start in different subbands that are shifted about each other. As a result, there is no unambiguous dependence of ΔE_{init} on $|\Delta N|$, which also causes the transition rate to lack a simple, single-valued dependence on ΔE_{init} .

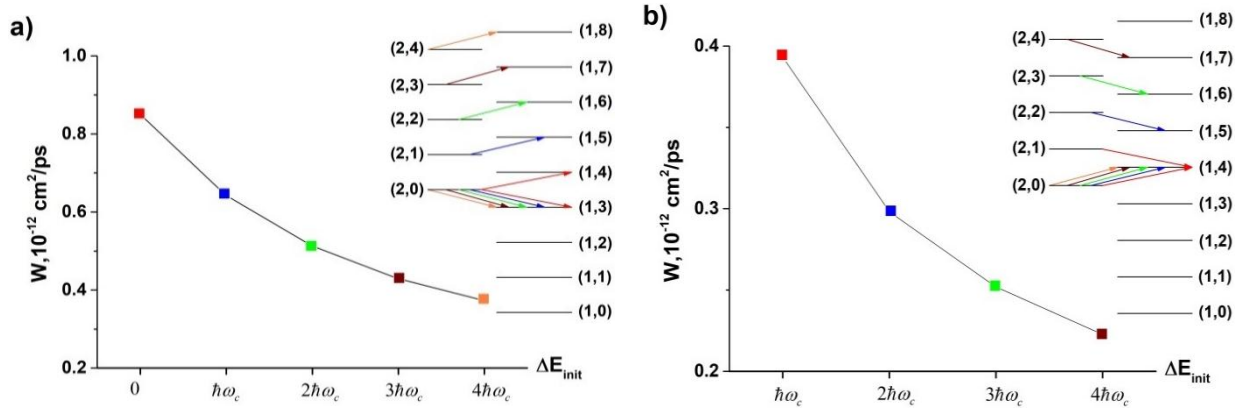


Figure 22. Dependence of the rate of inter-subband scattering of type I on the difference of initial values of the energy of electrons of the interacting pair ΔE_{init} . Magnetic field $B = 3.5$ T.

To illustrate the above, let us consider intrasubband transitions of type II at the value of the magnetic field when the Landau level (2,0) coincides with the level (1,3). Let consider the transition $\{(1,1 + \Delta N) \rightarrow (1, \Delta N) \& (2,0) \rightarrow (2,1)\}$. From the scheme of transitions in the inset to Figure 23, we can see that the ΔE_{init} decreases when ΔN is increasing from 1 to 3, and increases when ΔN is increasing further. As a result, for the first part of the transitions their rate decreases with increasing ΔN , and for the second part - increases.

It should be noted that the dependence on ΔN is weak for transitions of all types.

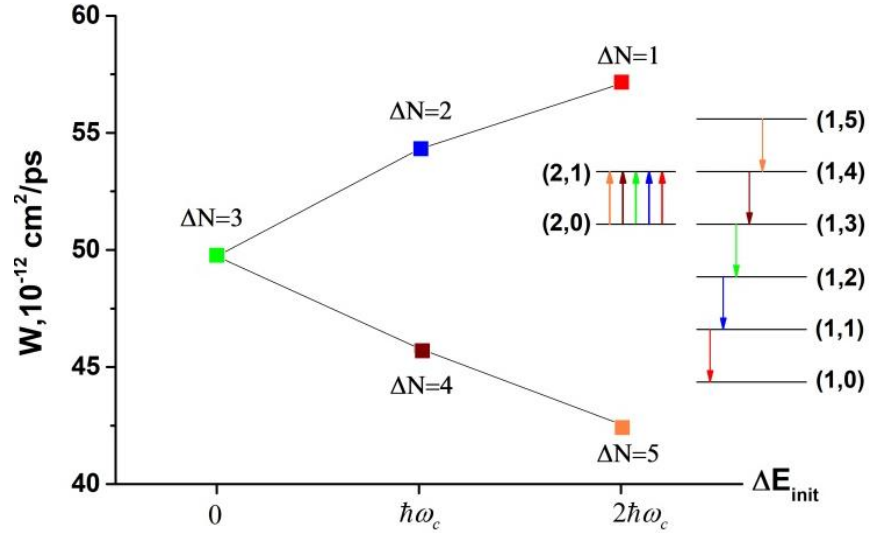


Figure 23. Dependence of the type II intra-subband scattering rate on the difference in the energy of the interacting pair of electrons before scattering. The magnetic field $B = 4.1 \text{ T}$ corresponds to the resonance when the Landau level (2,0) coincides with the Landau level (1,3).

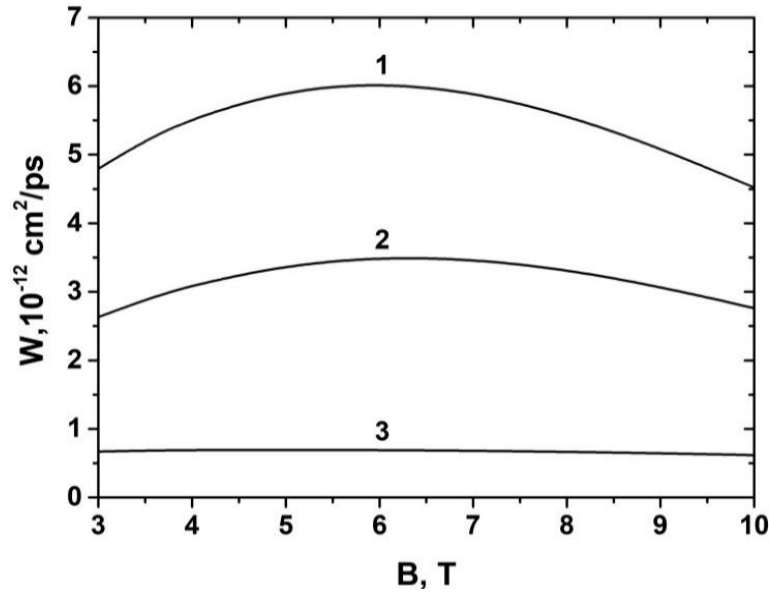


Figure 24. Dependence of the rate of type III transitions on the magnetic field strength.

1- $\{(2,0) \rightarrow (1,0) \& (1,4) \rightarrow (2,4)\}$, 2- $\{(2,2) \rightarrow (1,2) \& (1,6) \rightarrow (2,6)\}$,

3- $\{(2,0) \rightarrow (1,3) \& (1,4) \rightarrow (2,1)\}$.

For the intersubband transitions of type III, the resonance conditions have the same form (37) as for the intrasubband transitions. Therefore, the dependence of the rate of these transitions on the magnetic field strength is smooth (Fig. 24). The rate of type III transitions can reach values several times higher than the rate of type I intersubband

transitions while remaining an order of magnitude lower than the rate of intrasubband transitions.

In type II inter-subband transitions, resonance occurs when the Landau levels of the upper subband align with those of the lower subband. This alignment happens at specific magnetic field values defined by expression (45). As a result, the dependence of these transition rates on the magnetic field is a resonance peak.

The obtained expressions for the scattering rate enabled us to establish a selection rule for type II inter-subband transitions. This rule is defined by the symmetry of the quantum well's potential profile. In structures that have a symmetric profile, the scattering rate for all transitions $\{(\nu_i, n_i) \rightarrow (\nu_f, n_f) \& (\nu_j, n_j) \rightarrow (\nu_g, n_g)\}$ with an odd sum of subband numbers $\nu_i + \nu_j + \nu_g + \nu_f$ is zero.

Let us examine the change in the function $R_{\nu_i, \nu_j, \nu_g, \nu_f}(z_1)$ defined by expression (28) when the sign of the argument is altered.

$$R_{\nu_i, \nu_j, \nu_g, \nu_f}(-z_1) = \int_{-\infty}^{+\infty} dz_2 \varphi_{\nu_i}(z_2) \varphi_{\nu_j}(z_2 + 2z_1) \varphi_{\nu_g}^*(z_2 + 2z_1) \varphi_{\nu_f}^*(z_2). \quad (53)$$

Substituting the variable in the integral $z_2 \rightarrow -z_2$, we obtain

$$R_{\nu_i, \nu_j, \nu_g, \nu_f}(-z_1) = \int_{-\infty}^{+\infty} dz_2 \varphi_{\nu_i}(-z_2) \varphi_{\nu_j}(-z_2 + 2z_1) \varphi_{\nu_g}^*(-z_2 + 2z_1) \varphi_{\nu_f}^*(-z_2). \quad (54)$$

In structures with symmetric potential profile, the subband wave functions are divided by parity

$$\varphi_{\nu}(-z) = (-1)^{\nu+1} \varphi_{\nu}(z). \quad (55)$$

Substituting (55) into (54), we obtain

$$R_{\nu_i, \nu_j, \nu_g, \nu_f}(-z_1) = (-1)^{\nu_i + \nu_j + \nu_g + \nu_f} R_{\nu_i, \nu_j, \nu_g, \nu_f}(z_1). \quad (56)$$

Thus, in the case when the sum $\nu_i + \nu_j + \nu_g + \nu_f$ is odd, the function $R_{\nu_i, \nu_j, \nu_g, \nu_f}(z_1)$ is also odd, and, as a consequence, the integrand in the integral (27) defining the function $G_{\nu_i, \nu_j, \nu_g, \nu_f}(\gamma; y)$ is odd. Therefore, the function $G_{\nu_i, \nu_j, \nu_g, \nu_f}(\gamma; y)$ and, consequently, the rates of all transitions in which the sum of subband numbers $\nu_i + \nu_j + \nu_g + \nu_f$ is odd are equal to zero.

For type II transitions, when one of the electrons moves to a neighboring subband $\nu_i = \nu_j = \nu_f = \nu_g \pm 1$, and $\nu_i + \nu_j + \nu_g + \nu_f = 4\nu_i \mp 1$ is correspondingly odd.

Therefore, type II transitions between neighboring subbands are forbidden in structures with a symmetric profile. However, when it comes to transitions between subbands that are further apart (for example, between the first and the third), the intensity of these transitions is non-zero (see Fig. 25). Nonetheless, this intensity is nearly two orders of magnitude lower than that of type I inter-subband transitions. This difference is also attributed to the structure of wave functions in quantum wells with a symmetric potential profile, as illustrated in Figure 26, which displays the functions $R_{\nu_i, \nu_j, \nu_g, \nu_f}(z_l)$ associated with different types of transitions.

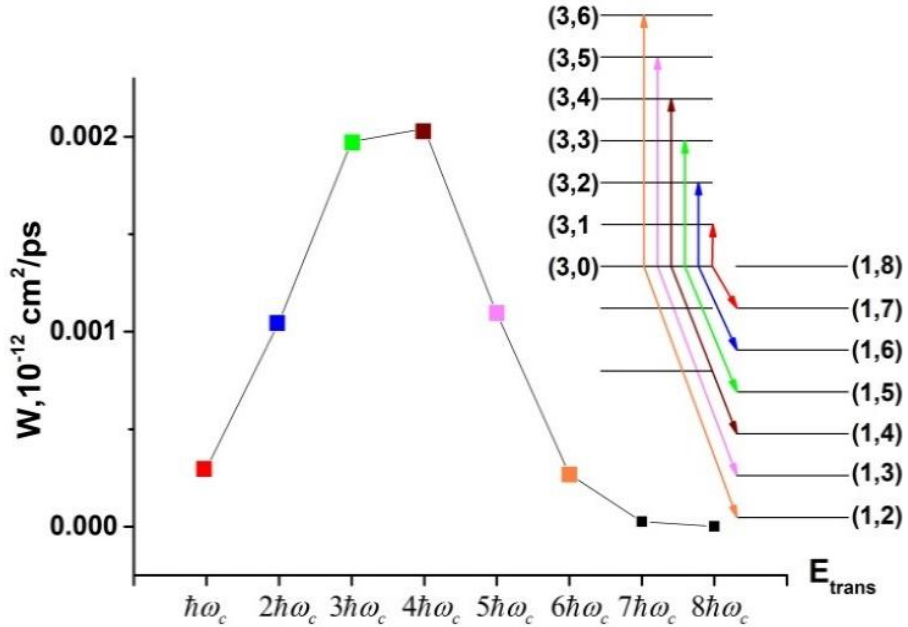


Figure 25. Dependence of the type II inter-subband transition rate on the energy transferred to one electron in the scattering event. The magnetic field $B=4.2$ T corresponds to the resonance when the Landau levels (3,0) and (1,8) coincide.

In structures with asymmetric potential profiles, the subband wave functions cease to have a certain parity ($\varphi_\nu(-z) \neq \varphi_\nu(z)$), resulting in non-zero probabilities for inter-subband transitions of type II. Consequently, the magnitude, behavior, and relative contribution of type II transitions depend significantly on the symmetry of the structure potential profile. Therefore, transitions of this type have to be investigated separately for each particular type of structure.

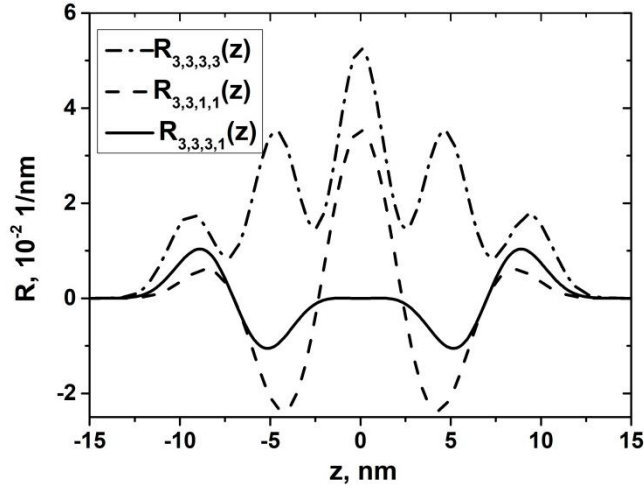


Figure 26. Function $R_{\nu_i, \nu_j, \nu_g, \nu_f}(z)$ for transitions of different types – intrasubband transitions in the third subband (dashed-dotted curve), inter-subband transitions of type I (dashed curve) and type II (solid curve) from the third to the first subband.

6. Effect of magnetic field orientation

In the case when the magnetic field has a component B_{\parallel} parallel to the layers of the quantum well, expression (13) gives the following resonance condition for the transition

$$\Delta \varepsilon_{if} + \delta \varepsilon_{if}(B_{\parallel}) + \Delta \varepsilon_{jg} + \delta \varepsilon_{jg}(B_{\parallel}) + (n_i - n_f + n_j - n_g) \cdot \hbar \omega_{\perp} = 0, \quad (57)$$

where

$$\delta \varepsilon_{if}(B_{\parallel}) = \frac{e^2}{2mc^2} \left[(\delta z)_{\nu_i}^2 - (\delta z)_{\nu_f}^2 \right] \cdot B_{\parallel}^2 \quad (58)$$

is the change in the distance between the ν_i -th and ν_f -th subbands due to the shift of each of the subbands as a whole, caused by B_{\parallel} . According to the oscillation theorem, the wave-function $\varphi_{\nu}(z)$ of the ν -th energy level contains $(\nu+1)$ zeros. Therefore, as ν increases, the complexity of the wave function also increases, leading to a larger root mean square (RMS) fluctuation $(\delta z)_{\nu}$ in the z -coordinate. Consequently, $\delta \varepsilon_{if}(B_{\parallel}) > 0$ if $\nu_i > \nu_f$, so when the magnetic field component B_{\parallel} increases, it causes a greater distance between the upper and lower subbands, as illustrated in Figure 27.

Since this shift of the subbands does not change their structure, it does not lead to a change in the resonance condition in the case where each of the electrons does not change its subband as a result of a scattering event. This is applicable for type I and type II intra-

subband transitions. For these transitions $\Delta\varepsilon_{if} = \Delta\varepsilon_{jg} = 0$ and $\delta\varepsilon_{if} = \delta\varepsilon_{jg} = 0$. As a result, the resonance condition in a tilted magnetic field remains the same as in a magnetic field that is perpendicular to the layers of the structure.

Neither does the resonance condition change for inter-subband transitions of type III. Although in this case $\delta\varepsilon_{if}(B_{\parallel})$ is nonzero for each of the electrons, however, $\Delta\varepsilon_{if} = -\Delta\varepsilon_{jg}$ and $\delta\varepsilon_{if}(B_{\parallel}) = -\delta\varepsilon_{jg}(B_{\parallel})$.

In the case of inter-subband transitions of type I and type II B_{\parallel} leads to a shift of their resonances (Fig. 28).

For the inter-subband transition $\{(\nu_i, n_i) \rightarrow (\nu_f, n_f) \& (\nu_i, n_j) \rightarrow (\nu_f, n_g)\}$ of type I, the condition (57) takes the following form

$$2\Delta\varepsilon_{if} + 2\delta\varepsilon_{if}(B_{\parallel}) - \frac{2\Delta\varepsilon_{if}}{\hbar\omega_{\perp}^{(0)}} \cdot \hbar\omega_{\perp} = 0, \quad (59)$$

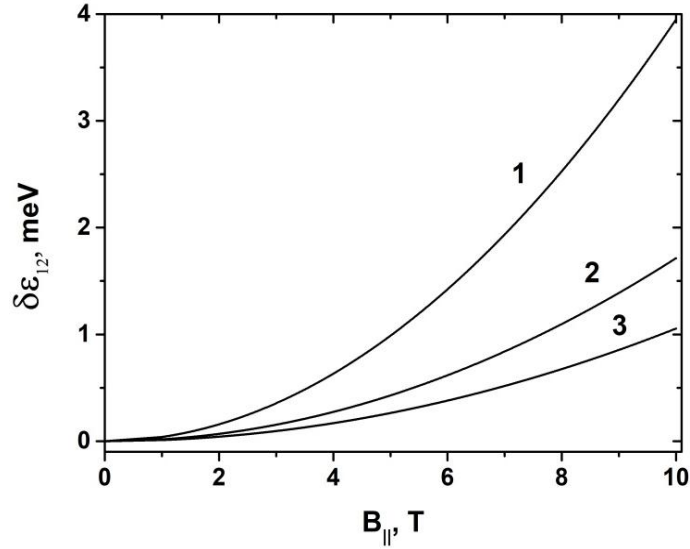


Figure 27. Dependence of the distance between two lowest subbands in a quantum well on the magnetic field component B_{\parallel} parallel to layers. Different curves correspond to different values of the quantum well width a : 1 - $a=25$ nm; 2 - $a=15$ nm; 3 - $a=10$ nm. The data are given for the quantum well GaAs/Al_{0.3}Ga_{0.7}As.

Here, we use the resonance condition (41) for this transition in perpendicular magnetic field, $\omega_{\perp}^{(0)} = \frac{eB_{\perp}^{(0)}}{mc}$, $B_{\perp}^{(0)}$ - the resonant value of perpendicular magnetic field

when $B_{\parallel} = 0$. From (59) we find the resonant value of the magnetic field component B_{\perp} , at which the resonance takes place if $B_{\parallel} \neq 0$:

$$\frac{B_{\perp}}{B_{\perp}^{(0)}} = 1 + \frac{\delta\epsilon_{if}(B_{\parallel})}{\Delta\epsilon_{if}} \quad (60)$$

Accordingly, the relative shift

$$\frac{\delta B_{\perp}}{B_{\perp}^{(0)}} = \frac{B_{\perp} - B_{\perp}^{(0)}}{B_{\perp}^{(0)}} = \frac{\delta\epsilon_{if}(B_{\parallel})}{\Delta\epsilon_{if}} \quad (61).$$

The relative shift in the magnetic field value at which the transition resonance occurs is independent of the Landau level numbers and is equal to the relative change in the inter-subband distance. As illustrated in Figure 29, the relative shift increases significantly as the width of the quantum well increases. This occurs because $\Delta\epsilon_{if}$ decreases while $\delta\epsilon_{if}(B_{\parallel})$ increases with an increase in the quantum well width. The increase in $\delta\epsilon_{if}(B_{\parallel})$ is caused by the growth of the localization area of the wave function, which, in turn, leads to a larger standard deviation δz for each of the subbands.

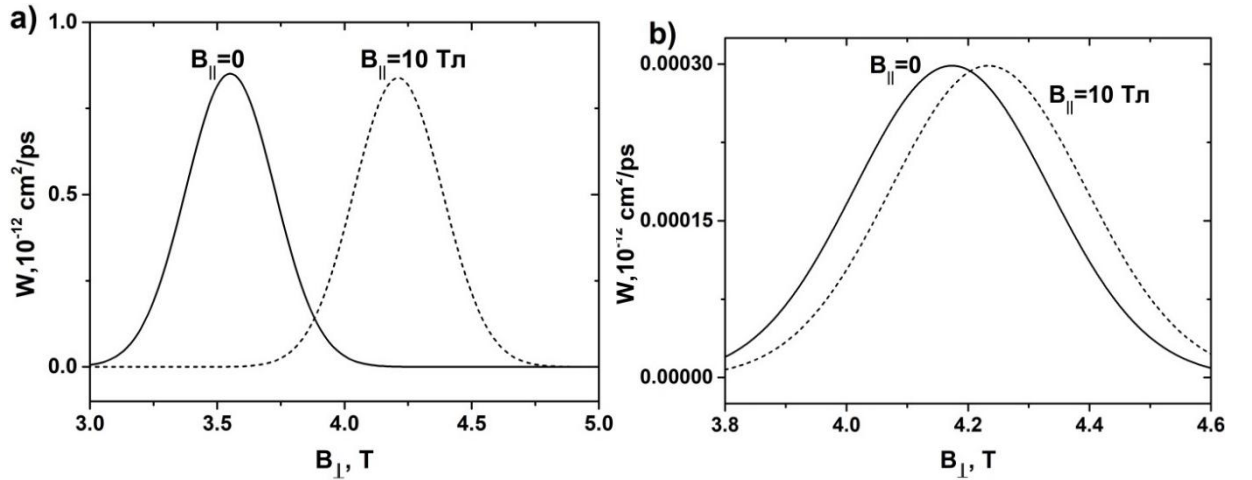


Figure 28. Effect of the magnetic field component B_{\parallel} parallel to the quantum well layers on the dependence of the electron-electron scattering rate for inter-subband transitions of type I (a) and type II (b) on the magnetic field component B_{\perp} perpendicular to the quantum well layers. The solid curve - $B_{\parallel} = 0$, the dashed curve - $B_{\parallel} = 10 \text{ T}$. The data are given for the transition $\{(2,0) \rightarrow (1,3) \& (2,0) \rightarrow (1,4)\}$ (a) and $\{(3,0) \rightarrow (3,1) \& (3,0) \rightarrow (1,7)\}$ (b) in GaAs/Al_{0.3}Ga_{0.7}As quantum well of 25 nm width.

To estimate the effect, let us consider deep levels in a rectangular quantum well with width a , where most of the wave function is located within the well. Thus, we can neglect the penetration of the wave function into the barrier and consider the quantum well as infinitely deep. Then we obtain

$$(\delta z)_\nu^2 = \frac{a^2}{12} \left(1 - \frac{6}{(\pi\nu)^2} \right), \quad (62)$$

and

$$\delta\epsilon_{if}(B_\parallel) = \frac{e^2}{4\pi^2 mc^2} \left[\frac{1}{\nu_f^2} - \frac{1}{\nu_i^2} \right] \cdot a^2 \cdot B_\parallel^2 \quad (63)$$

Correspondingly, for the relative magnitude of the resonance shift, we have

$$\frac{\delta B_\perp}{B_\perp^{(0)}} = \frac{B_\perp - B_\perp^{(0)}}{B_\perp^{(0)}} = \frac{\delta\epsilon_{if}(B_\parallel)}{\Delta\epsilon_{if}} \frac{e^2}{2\pi^4 c^2 \hbar^2} \frac{1}{\nu_i^2 \nu_f^2} \cdot a^4 \cdot B_\parallel^2. \quad (64)$$

Thus, the relative shift of the resonance grows as the fourth power of the quantum well width.

It follows from (61) that the resonance at the transition from the upper subband to the lower one shifts in the direction of higher magnetic fields and has the value of

$$\delta B_\perp = \frac{mc}{e\hbar} \frac{2\delta\epsilon_{if}(B_\parallel)}{n_f + n_g - n_i - n_j} = \frac{e}{\hbar c} \frac{[(\delta z)_{\nu_i}^2 - (\delta z)_{\nu_f}^2]}{n_f + n_g - n_i - n_j} \cdot B_\parallel^2 \quad (65).$$

As can be seen from (65), the magnitude of the shift is proportional to the increment of the inter-subband distance and, accordingly, grows with increasing quantum well width approximately as the square of the width (Fig. 30).

The shifts of resonances depend rather strongly (quadratically) on B_\parallel , which makes it possible for this component to significantly influence both the magnitude of type I inter-subband scattering rates and the ratio of rates of various transitions. As a result, some transitions are considerably suppressed, while the rate of others is notably increased (see Fig. 31).

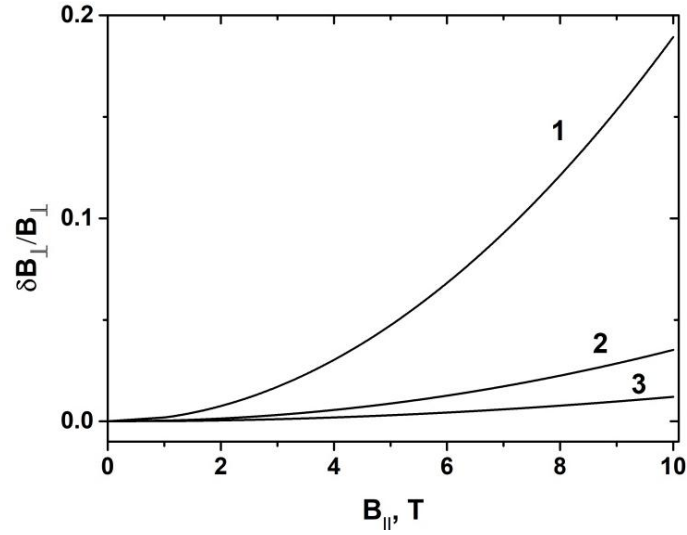


Figure 29. Dependence of the relative shift of the type I transition resonance between the lowest subbands on the magnetic field component B_{\parallel} parallel to the layers of the quantum well. Different curves correspond to different values of the width a of the quantum well: 1 - $a=25$ nm; 2 - $a=15$ nm; 3 - $a=10$ nm.

For the inter-subband transition $\{(\nu_i, n_i) \rightarrow (\nu_f, n_f) \& (\nu_i, n_j) \rightarrow (\nu_i, n_g)\}$ of type II, the resonance condition (57) takes the form

$$\Delta\epsilon_{if} + \delta\epsilon_{if}(B_{\parallel}) - \frac{\Delta\epsilon_{if}}{\hbar\omega_{\perp}^{(0)}} \cdot \hbar\omega_{\perp} = 0. \quad (66)$$

Here, the resonance condition for $B_{\parallel} = 0$ is taken into account:

$$\frac{\Delta\epsilon_{if}}{\hbar\omega_{\perp}^{(0)}} = (n_f - n_i + n_g - n_j). \quad (67)$$

It follows from (66) that the relations (60) and (61) are also valid for inter-subband transitions of type II, from which, taking into account (67), we find

$$\delta B_{\perp} = \frac{mc}{e\hbar} \frac{\delta\epsilon_{if}(B_{\parallel})}{n_f + n_g - n_i - n_j} = \frac{e}{2\hbar c} \frac{[(\delta z)_{\nu_i}^2 - (\delta z)_{\nu_f}^2]}{n_f + n_g - n_i - n_j} \cdot B_{\parallel}^2 \quad (68)$$

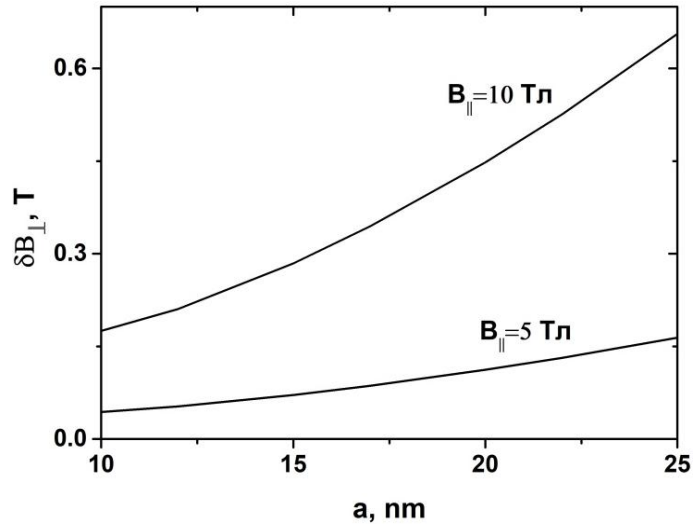


Figure 30. Dependence of the resonance shift of the inter-subband transition of type I in tilted magnetic field on the quantum well width. The data are given for the transition $\{(2,0) \rightarrow (1,3) \& (2,0) \rightarrow (1,4)\}$.

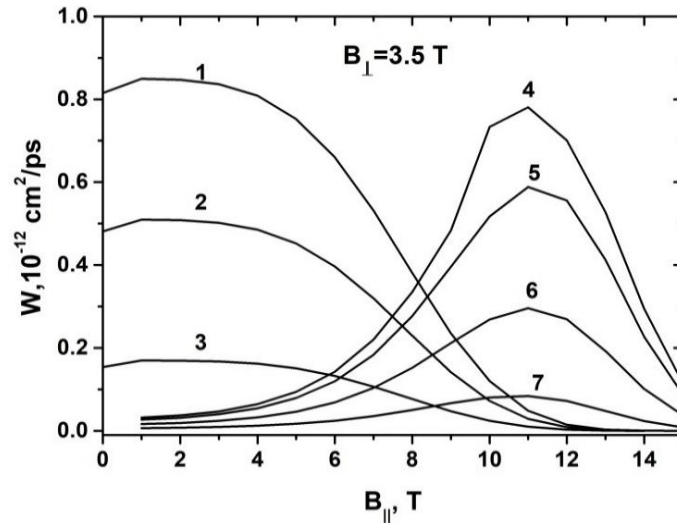


Figure 31. Dependence of the transition rate on B_{\parallel} at the fixed value of $B_{\perp} = 3.5$ T.

- 1 - $\{(2,0) \rightarrow (1,3) \& (2,0) \rightarrow (1,4)\}$; 2 - $\{(2,0) \rightarrow (1,2) \& (2,0) \rightarrow (1,5)\}$;
 3 - $\{(2,0) \rightarrow (1,1) \& (2,0) \rightarrow (1,6)\}$; 4 - $\{(2,0) \rightarrow (1,4) \& (2,0) \rightarrow (1,4)\}$;
 5 - $\{(2,0) \rightarrow (1,3) \& (2,0) \rightarrow (1,5)\}$; 6 - $\{(2,0) \rightarrow (1,2) \& (2,0) \rightarrow (1,6)\}$;
 7 - $\{(2,0) \rightarrow (1,1) \& (2,0) \rightarrow (1,7)\}$.

The component B_{\parallel} enters expression (25) for the scattering rate amplitude only through the parameter ξ , which is determined by expression (34). In electron-electron scattering, two electrons change their states, resulting in two associated parameters in the scattering amplitude: ξ_{ν_f, ν_i} corresponding to the transition of the first electron and ξ_{ν_g, ν_j} for the second electron. When both parameters are zero ($\xi_{\nu_f, \nu_i} = \xi_{\nu_g, \nu_j} = 0$), the scattering

rate is independent on B_{\parallel} . This parameter is proportional to the difference between the average coordinates $\langle z \rangle_{\nu} = \int dz |\phi_{\nu}(z)|^2 z$ in the initial and final states of the electron. If the average coordinates are the same, the parameter ξ becomes zero.

In the case of intra-subband scattering processes of type I $\nu_i = \nu_j = \nu_g = \nu_f$. Accordingly, $\xi_{\nu_f, \nu_i} = \xi_{\nu_g, \nu_j} = 0$, and hence the scattering rate amplitude of any intra-subband transition of type I is independent of the magnetic field component B_{\parallel} . At the same time, the resonance condition is also independent on B_{\parallel} .

In type II intra-subband scattering processes, the electrons occupy different subbands. However, after scattering, each electron remains in the same subband it initially occupied, i.e., $\nu_f = \nu_i$ and $\nu_g = \nu_j$. Accordingly, $\langle z \rangle_{\nu_f} = \langle z \rangle_{\nu_i}$ and $\langle z \rangle_{\nu_g} = \langle z \rangle_{\nu_j}$. Then $\xi_{\nu_f, \nu_i} = \xi_{\nu_g, \nu_j} = 0$, and the amplitude of the scattering rate of any type II intra-subband transition is also independent on B_{\parallel} . Moreover, the resonance condition for any transition of this type does not depend on B_{\parallel} .

Thus, in the case of intra-subband scattering processes, the magnetic field component parallel to the structure layers does not affect electron-electron scattering processes.

The effect of the component B_{\parallel} on the amplitude of inter-subband transitions is determined by the symmetry of the potential profile of the structure $U(z)$. In the case of a symmetric potential profile ($U(-z) = U(z)$) the wave-functions of the subbands exhibit either even or odd symmetry. Therefore, the average coordinates for all Landau levels across the subbands are identical. Hence, for all transitions $\xi_{\nu_f, \nu_i} = \xi_{\nu_g, \nu_j} = 0$.

Thus, we conclude that in quantum wells with a symmetric potential profile, the amplitude A_{e-e} of transitions of all types is independent on B_{\parallel} . The effect of this component of the magnetic field is manifested only in the shift of the resonances of inter-subband transitions of types I and II to higher (transitions from the upper subband to the lower subband) or lower (transitions from the lower subband to the upper subband) values of the quantising component B_{\perp} of the magnetic field. When the resonances are

shifted, the maximum value of the scattering rate changes slightly due to the dependence of the amplitude A_{e-e} on B_{\perp} (Fig. 32).

In the case of an asymmetric potential profile, the subband wave-functions $\varphi_{\nu}(z)$ are not divided by parity. This means that the average coordinates $\langle z \rangle$ in the initial and final states of one (for type II) or both (type I and type III) interacting electrons differ. As a result, one or both parameters ξ would be nonzero, and the transition amplitude A_{e-e} would depend both on B_{\perp} , and on B_{\parallel} .

The asymmetry of the potential profile can be achieved either by applying an external field, such as an electric field [9], or by designing an asymmetric quantum well structure itself [30,31]. Expression (25) indicates that the dependence of the scattering rate amplitude on ξ is non-monotonic. Altering the potential profile to change ξ results in changes to the subband wave-functions. These wave-functions influence the amplitude not only through the parameter ξ , but also via the integral $R_{\nu_i, \nu_j, \nu_g, \nu_f}(z)$. Consequently, the behavior of the amplitude in response to changes in the potential is quite complex and ambiguous; therefore, it should be examined individually configuration of the structure.

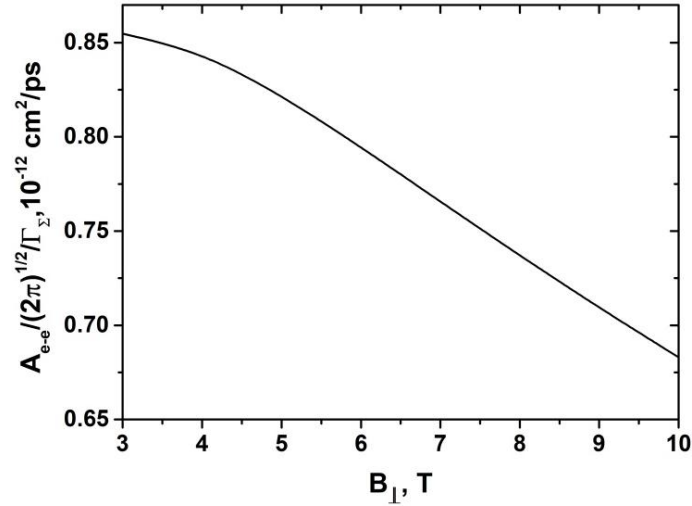


Figure 32. Dependence of $A_{e-e} / (\sqrt{2\pi} \Gamma_{\Sigma})$ on B_{\perp} . Data are given for the transition $\{(2,0) \rightarrow (1,3) \& (2,0) \rightarrow (1,4)\}$ for $GaAs / Al_{0.3}Ga_{0.7}As$ quantum well of 25 nm width.

In conclusion, we note that our numerical calculations accounted for the nonparabolicity of the subbands. We considered band nonparabolicity according to the theory outlined in reference [32], applying second-order perturbation theory and including terms in the dispersion law expansion up to the fourth order of the wave vector.

We considered transitions from Landau levels that are below the optical phonon energy up to magnetic field values where only two Landau levels of the lower subband remain below the optical phonon level. We found no significant effect of the band nonparabolicity on the electron-electron scattering rates.

7. Conclusion

Through analytical transformations, we significantly reduced the complexity of the integral in the expression for the electron-electron scattering rate between Landau levels in a quantum well structure. This enabled us to calculate the “complete” matrix of electron-electron scattering rates and to analyze all types of transitions, both intra-subband and those occurring between the Landau levels of different subbands.

We found that the intra-subband electron-electron scattering rate exhibits a relatively weak dependence on the energy difference of the electrons in the initial state. As a result, the scattering rates for transitions where the electrons start at the same level are close to the rates for transitions where the electrons begin at levels that are a rather far from each other on the Landau level ladder. Additionally, the rates of intra-subband type II transitions, caused by the interaction of electrons in different subbands, are comparable in magnitude and can even exceed the scattering rates when both electrons in the interacting pair are at the same Landau level.

It is shown that in intra-subband scattering there is a rapid monotonic decrease of the scattering rate with increasing energy transferred to the electron in the scattering event. In contrast, such dependence for electron-electron scattering between subbands is ambiguous. Depending on the specific type of the inter-subband transitions and initial Landau levels of electrons in the interacting pair, the scattering rate can either decrease or increase monotonically, and it is also possible to observe non-monotonic dependence of the scattering rate on the transferred energy.

The expression for the electron-electron scattering rate in a quantizing magnetic field, tilted with respect to the plane of the quantum well layers, was derived for a case when the cyclotron energy is lower than the intersubband spacing.

It was demonstrated that, across a wide range of magnetic field strengths, the component of the magnetic field that is parallel to the structure layers does not significantly affect the intra-subband electron-electron scattering rates.

Two aspects can be specified regarding the impact of the parallel-to-layers magnetic field component on inter-subband scattering.

The first aspect is the effect on the form factor, which is determined by the energy spectrum. The resonance of type I and type II inter-subband transitions shifts to other values of the magnetic field due to the increase of the inter-subband distance in tilted magnetic field. Meanwhile, the parallel component of the magnetic field does not change the resonance conditions for type III transitions.

The second aspect involves the effect of B_{\parallel} on the amplitude of inter-subband transitions. This amplitude does not directly depend on energy but is influenced by the wave functions. It was demonstrated that the nature of this effect is determined by the symmetry of the potential profile of the quantum well structure. In structures with a symmetric potential profile, the effect of B_{\parallel} is nearly absent. However, in cases with an asymmetric potential profile, the amplitude is dependent on both B_{\perp} and B_{\parallel} .

References

- [1] T. Ando, B. Fowler, F. Stern, Rev. Mod. Phys. **54**, 437 (1982).
DOI: <https://doi.org/10.1103/RevModPhys.54.437>
- [2] A. Blank, and S. Feng, J. Appl. Phys. **74**, 4795 (1993).
DOI: <https://doi.org/10.1063/1.354354>
- [3] D. Smirnov, O. Drachenko, J. Leotin, H. Page, C. Becker, C. Sirtori, V. Apalkov, and T. Chakraborty. Phys. Rev. B **66**, 125317 (2002).
DOI: <https://doi.org/10.1103/PhysRevB.66.125317>
- [4] K. Kempa, Y. Zhou, J. R. Engelbrecht, and P. Bakshi. Phys. Rev. B **68**, 085302 (2003).
DOI: <https://doi.org/10.1103/PhysRevB.68.085302>
- [5] C. Becker, A. Vasanelli, C. Sirtori, and G. Bastard. Phys. Rev. B **69**, 115328 (2004).
DOI: <https://doi.org/10.1103/PhysRevB.69.115328>
- [6] A. Leuliet, A. Vasanelli, A. Wade, G. Fedorov, D. Smirnov, G. Bastard, and C. Sirtori. Phys. Rev. B **73**, 085311 (2006).
DOI: <https://doi.org/10.1103/PhysRevB.73.085311>

- [7] I. Savić, Z. Ikonić, V. Milanović, N. Vukmirović, V.D. Jovanović, D. Indjin, and P. Harrison. Phys. Rev. B **73**, 075321 (2006).
DOI: <https://doi.org/10.1103/PhysRevB.73.075321>
- [8] B. Novaković, J. Radovanović, A. Mirčetić, V. Milanović, Z. Ikonić, and D. Indjin. Opti. Commun. **279**, 330 (2007).
DOI: <https://doi.org/10.1016/j.optcom.2007.07.028>
- [9] M.P. Telenkov, Yu.A. Mityagin, and P.F. Kartsev. JETP Lett. **92**, 401 (2010).
DOI: <https://doi.org/10.1134/S0021364010180086>
- [10] D. Timotijević, J. Radovanović, and V. Milanović. Semicond. Sci. Technol. **27**, 045006 (2012).
DOI: <https://doi.org/10.1088/0268-1242/27/4/045006>
- [11] M. P. Telenkov, Yu. A. Mityagin, P.F. Kartsev. Opt. Quant. Electron. **46**, 759 (2014).
DOI: <https://doi.org/10.1007/s11082-013-9784-z>
- [12] M.P. Telenkov, Yu.A. Mityagin, A.A. KutsevolV.V. Agafonov, and K.K. Nagaraja. JETP Letters **102**, 678 (2015).
DOI: <https://doi.org/10.1134/S0021364015220129>
- [13] M.P. Telenkov, Yu.A. Mityagin, T.N.V. Doan, and K.K. Nagaraja. Physica E **104**, 11 (2018).
DOI: <https://doi.org/10.1016/j.physe.2018.07.007>
- [14] Yu.A. Mityagin, M.P. Telenkov, Sh. Amiri, K.K. Nagaraja, Physica E **122**, 114104 (2020).
DOI: <https://doi.org/10.1016/j.physe.2020.114104>
- [15] Yu.A. Mityagin, M.P. Telenkov; I.A. Bulygina, Ravi Kumar, K.K. Nagaraja, Physica E **142**, 115288 (2022).
DOI: <https://doi.org/10.1016/j.physe.2022.115288>
- [16] M.P. Telenkov; Yu.A. Mityagin, Resonant tunneling transport in superlattices, Chapter 3, pp. 74-95, Lambert Academic Publishing GmbH & Co, KG, Saarbrücken, Germany, 2011.
- [17]. G.M.G. Oliveira, V.M.S. Gomes, A.S. Chaves, J.R. Leite, and J.M. Worlock. Phys.Rev. B **35**, 2896 (1987).
DOI: <https://doi.org/10.1103/PhysRevB.35.2896>
- [18]. S. Živanović, V. Milanović, and Z. Ikonić. Phys. Rev. B **52**, 8305 (1995).

DOI: <https://doi.org/10.1103/PhysRevB.52.8305>

[19] G. Bastard. Wave Mechanic Applied to Semiconductor Heterostructures. Les Editions de Physique, Les Ulis Cedex, France, 1988.

[20] D. M. Mitrinović, V. Milanović, and Z. Ikonić. Phys. Rev. B **54**, 7666 (1996).

DOI: <https://doi.org/10.1103/PhysRevB.54.7666>

[21] V.V. Kapaev, Yu.V. Kopaev, and I.V. Tokatly, Physics - Uspekhi **40**, 538 (1997).

DOI: <https://doi.org/10.1070/PU1997v040n05ABEH001568>

[22] M.P. Telenkov and Yu.A. Mityagin. Semiconductors **40**, 581 (2006).

DOI: <https://doi.org/10.1134/S1063782606050125>

[23] J. Hu and A. H. MacDonald. Phys. Rev. B **46**, 12554 (1992).

DOI: <https://doi.org/10.1103/PhysRevB.46.12554>

[24] S.K. Lyo, N.E. Harff, and J.A. Simmons. Phys. Rev. B **58**, 1572 (1998).

DOI: <https://doi.org/10.1103/PhysRevB.58.1572>

[25] M. L. Leadbeater, F.W. Sheard, and L. Eaves. Semicond. Sci. Technol. **6**, 1021 (1991).

DOI: <https://doi.org/10.1088/0268-1242/6/10/012>

[26] M.P. Telenkov, Yu.A. Mityagin, T.N.V. Doan, and K.K. Nagaraja. J. Phys. Commun. **2**, 085019 (2018).

DOI: <https://doi.org/10.1088/2399-6528/aad885>

[27] T. Uenoyama and L J. Sham. Phys. Rev. B **39**, 11044 (1989).

DOI: <https://doi.org/10.1103/PhysRevB.39.11044>

[28] S.K. Lyo. Phys. Rev. B **57**, 9114 (1998).

DOI: <https://doi.org/10.1103/PhysRevB.57.9114>

[29] G. Bastard, E. E. Mendez, L. L. Chang, and L. Esaki. Phys. Rev. B **26**, 1974 (1982).

DOI: <https://doi.org/10.1103/PhysRevB.26.1974>

[30] M. P. Telenkov, Yu. A. Mityagin, P.F. Kartsev. Nanoscale Res Lett. **7**, 491 (2012).

DOI: <https://doi.org/10.1186/1556-276X-7-491>

[31] M.P. Telenkov, Yu.A. Mityagin, A.A. KutsevoI.V. Agafonov, and K.K. Nagaraja. JETP Letters, **100**, 644 (2015).

DOI: <https://doi.org/10.1134/S0021364014220184>

[32] U. Ekenberg. Phys. Rev. B **40**, 7714 (1989)

DOI: <https://doi.org/10.1103/PhysRevB.40.7714>